Review | Open Access

Microstructures

Chen *et al. Microstructures* **2026**, *6*, 2026091 **DOI:**10.20517/microstructures.2025.170

Advancements in porous organic frameworks based electrochemical sensors for organophosphorus pesticides detection

Zihang Chen[1], Sijie Ma[1], Ting Yao[1], Haiying He[1], Ting Fan[1], Yi Yu[2], Suo Wang[3], Liangbin Xiong[4], Xiaodong Hong[1], Guangjin Wang[1]

Keywords:
Porous organic frameworks, metal-organic frameworks, covalent organic frameworks, electrochemical sensors, organophosphorus pesticides

Citation: Chen, Z.; Ma, S.; Yao, T.; He, H.; Fan, T.; Yu, Y.; Wang, S.; Xiong, L.; Hong, X.; Wang, G. Advancements in porous organic frameworks based electrochemical sensors for organophosphorus pesticides detection. *Microstructures* **2026**, *6*, 2026091. https://dx.doi.org/10.20517/microstructures.2025.170

Received: 21 Dec 2025 **First Decision:** 27 Feb 2026 **Revised:** 19 Apr 2026 **Accepted:** 22 May 2026 **Published:** 3 Jul 2026

Academic Editor: Zaiping Guo
Copy Editor: Shu-Yuan Duan
Production Editor: Shu-Yuan Duan

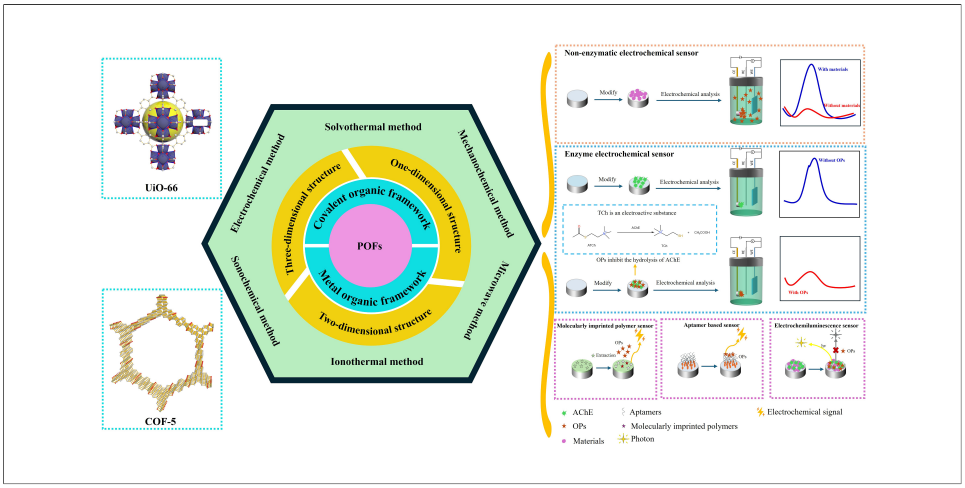

Abstract

Covalent organic frameworks (COFs) and metal-organic frameworks (MOFs), two important classes of crystalline porous organic frameworks (POFs), are constructed from organic structural units for COFs, and metal ions/clusters coordinated with organic ligands for MOFs, via robust chemical bonds. Due to their outstanding physicochemical properties, including large specific surface area, favorable structural stability, excellent biocompatibility and high porosity, POFs have gained considerable attention in the domain of electrochemical sensing of organophosphorus pesticides (OPs). Through the persistent endeavors of researchers, the construction of POFs-based electrochemical sensors for detecting OPs has made significant advances. Accordingly, this review introduces the dimensional classifications of POFs (one-, two- and three-dimensional POFs), and summarizes the six typical preparation methods to further realize the controllable synthesis of POFs with tunable compositions and structures. More importantly, the research advances in the fabrication of POFs-based non-enzymatic/enzymatic electrochemical sensors and their electrochemical performance for the detection of OPs

[1]School of Materials and Energy, Foshan University, Foshan 528000, Guangdong, China.
[2]Hubei Key Laboratory of Advanced Technology for Automotive Components, Wuhan University of Technology, Wuhan 430070, Hubei, China.
[3]The Fifth Electronic Research Institute of the Ministry of Industry and Information Technology, Guangzhou 510000, Guangdong, China.
[4]School of Optoelectronic Engineering, Guangdong Polytechnic Normal University, Guangzhou 510665, Guangdong, China.

Correspondence to: Assoc. Prof. Yi Yu, Hubei Key Laboratory of Advanced Technology for Automotive Components, Wuhan University of Technology, Wuhan 430070, Hubei, China. E-mail: yuyiwhut08@whut.edu.cn; Prof. Xiaodong Hong, Prof. Guangjin Wang, School of Materials and Energy, Foshan University, Foshan 528000, Guangdong, China. E-mail: hongxiaodong@lntu.edu.cn;

wangguangjin@whut.edu.cn

are emphatically reviewed. In addition, the research progress of other POFs-based electrochemical sensors, including molecularly imprinted polymer (MIP), aptamer based (APT) and electrochemiluminescence (ECL) sensors for the detection of OPs, is also briefly presented. Finally, the prospective research directions for developing high-performance POFs-based electrochemical sensors are outlined to facilitate the accurate, quick, efficient and economical real-time detection of OPs in food matrices.

INTRODUCTION

In October 2025, the Nobel Prize in Chemistry was granted to Susumu Kitagawa (Kyoto University), Richard Robson (University of Melbourne) and Omar M. Yaghi (University of California, Berkeley) by the Royal Swedish Academy of Sciences, in recognition of their groundbreaking achievements in the development of metal-organic frameworks (MOFs) or porous coordination polymers (PCPs)[1]. It is well known that MOFs are formed by the connection of organic ligands and metal ions (or clusters) through coordination bonds, and belong to the category of crystalline porous organic frameworks (POFs)[2,3]. Additionally, in the absent of metal elements, organic structural units are directly linked to each other by robust covalent bonds to form another class of crystalline POFs, known as COFs[4]. Compared with conventional inorganic porous materials including zeolites and molecular sieves, POFs have multiple unique features[5-7]: (1) long range order, well-defined crystalline structure and topological framework; (2) large specific surface area and tunable porosity; (3) versatile structure design and surface functionalization; (4) diverse enzyme-like biocatalytic activity; (5) excellent biocompatibility. Owing to these distinctive structural features, POFs as sensing platform for detection of food contaminants has attracted widespread attention in the field of food safety.

As one of the most common food contaminants, pesticides are utilized to manage or eradicate crop diseases and insect pests, thus improving crop yield and quality, thereby mitigating the global food crisis exacerbated by population growth[8]. According to their chemical structures, pesticides are categorized into organophosphorus, organochlorine, carbamate, pyrethroid, cypermethrin and others[9]. Among them, the application of organophosphorus pesticides (OPs) constitutes over 30% of global pesticide consumption, on account of their low cost, degradability and high efficacy against diverse pests[10]. Nevertheless, excessive application of OPs has resulted in the contamination of food matrices. After contaminated food matrices are ingested by human body, residual OPs inactivate acetylcholinesterase (AChE) and other neuropathy target esterases, thereby inhibiting the decomposition of acetylcholine (ACh), causing the disorders of reproductive, endocrine or nervous system, and even death[11]. Consequently, the development of precise, quick, efficient and economical detection technologies for monitoring OPs residue level in food matrices is significant for human health.

Compared with traditional complicated and time-consuming analytical technologies such as gas chromatography[12], gas chromatography-mass spectrometry[13], liquid chromatography-mass spectrometry[14], immunoassay[15] and colorimetry[16], electrochemical sensing technologies have many merits, including low cost, high selectivity, excellent sensitivity and facile rapid real-time detection[17]. It is well known that the physicochemical properties of the working electrode materials in electrochemical sensors directly determine their detection performance[18-21]. Due to their inherent large specific surface area, abundant catalytic active sites, outstanding conductivity, high porosity and structural stability, POFs have received much attention as working electrode materials for constructing electrochemical sensors for OPs detection[22,23]. For instance, Wang *et al.*[23] reported that the limit of detection (LOD) of electrochemical sensors based on COFs nanofibers (NFs) for dichlorvos was 0.11 μM under optimized detection conditions. Additionally, Duan *et al.*[22] found that the LOD of curcumin modified MOFs-based electrochemical sensors for methyl parathion

was 0.98 ng mL-1 under optimal detection conditions. These remarkable findings demonstrate that POFs-based electrochemical sensors have tremendous application potential in OPs detection. Consequently, extensive efforts have been dedicated to fabricating POFs-based electrochemical sensors for monitoring OPs in food matrices.

In 2021, Nangare *et al.*[24] reviewed the relationship between the spatial structures of MOFs and their physicochemical properties and discussed the sensitivity and selectivity of several MOFs-based sensors, including electrochemical, fluorescent and colorimetric sensors. Afterwards, Zhang *et al.*[10] summarized the preparation methods, detection mechanisms and practical applications of multiple MOFs-based sensors, including fluorescent, electrochemical, surface-enhanced Raman spectroscopy, electrochemiluminescence and colorimetric sensors. In addition, Lu *et al.*[25] analyzed the application status of COFs-based electrochemical sensors for monitoring various food contaminations and discussed the modification strategies for their electrochemical detection properties. Through the continuous efforts of researchers, the construction of POFs-based electrochemical sensors for OPs detection has made significant new progress in the past few years. However, there is a lack of systematic summaries regarding these progresses. Herein, the dimensional categories of POFs and their typical synthesis methods will be briefly introduced. Then, the non-enzymatic and enzymatic electrochemical sensing applications of POFs in OPs detection will be emphatically reviewed. Simultaneously, POFs-based electrochemical-related sensors, such as molecularly imprinted polymer (MIP), APT and ECL sensors will be discussed in brief. Finally, the potential research orientations for the construction of electrochemical sensors based on POFs for detecting will be outlined.

CLASSIFICATIONS OF POFS

It is well known that POFs are one of the important crystalline reticular structure materials, including hydrogen-bonded organic frameworks (HOFs), COFs and MOFs[26]. Among them, HOFs are assembled from organic molecules via hydrogen-binding interactions. As the hydrogen bond energy in HOFs is weaker than that of covalent bonds in COFs and coordination bonds in MOFs, HOFs exhibit lower stability than COFs and MOFs. Due to their insufficient stability, HOFs have not yet been used for detecting OPs in food matrices. Accordingly, only COFs and MOFs will be discussed in the following section. Benefiting from the diversity spatial conformations of functional groups in organic structural units or organic ligands, these two categories of POFs can form structures with different dimensions.

Up to now, numerous one-dimensional COFs and MOFs have been successfully prepared by various synthetic strategies[27,28]. These one-dimensional POFs exhibit large dimension along a special growth direction, displaying as tube-like, chain-like or rod-like structures. The high porosity and large surface area of one-dimensional POFs provide them abundant available catalytic active sites, enabling their application in various electrochemical reactions[29]. Unfortunately, one-dimensional COFs have not yet been employed for the detection of food containments, and only a few studies have explored the application of one-dimensional MOFs in food contaminants detection. For example, Pezhhanfar *et al.*[30] employed one-dimensional iron-gallic acid MOFs prepared by a solvothermal method to simultaneously extract and concentrate multiple pesticides, including fenitrothion, acetochlor, fenoxaprop-P-ethyl, difenoconazole and haloxyfop-R-methyl in watermelon juice and flesh samples.

More importantly, a large number of two-dimensional and three-dimensional POFs have been prepared and employed to monitor food contaminants. Therefore, to obtain high-performance POFs for the detection of food contaminants, the dimensional features of these two types of POFs are discussed in detail. For two-dimensional POFs, in the absence of metal ions, flaky organic structural units are π-π stacked to form two-dimensional COFs[31]. Their robust covalent interactions endow two-dimensional COFs with outstanding

chemical and electrochemical structural stability and excellent electronic conductivity, but the formation of small void spaces limits mass transfer within the planes and one-dimensional channels. To date, most of the as-prepared COFs possess a two-dimensional structure. Unlike stable COFs, single layers containing metal ions as nodes are stacked by weak interactions along the z-axis to construct two-dimensional MOFs. Owing to their weak non-covalent interactions, the ordered and open channels of two-dimensional MOFs are controllably regulated by the chosen of organic ligands and metal ions[32]. Their optimizable porous structures endow two-dimensional MOFs with rapid mass transfer properties, which is conducive to promoting their application in electrochemical sensing for the detection of food contaminants.

Additionally, for three-dimensional POFs, in the absence of metal ions, four- and six-linked three-dimensional organic structural units are connected to each other to construct π-conjugated three-dimensional COFs with interlaced channels[33], thus endowing three-dimensional COFs abundant electrochemical catalytic active sites. As compare to two-dimensional COFs, three-dimensional COFs exhibit much lower uniformity and crystallinity, leading to insufficient electronic conductivity and an unstable crystalline structure. Simultaneously, the limited chosen of three-dimensional organic structural units hinders the structural diversity of three-dimensional COFs[34]. In contrast, three-dimensional MOFs are constructed through robust coordination interactions between organic ligands and metal ions (or clusters), giving three-dimensional MOFs high structural stability as well as well-defined pore structure and size[35]. However, the exposed electrochemical catalytic active sites of three-dimensional MOFs still need to be further improved for expand their application scope, compared with two-dimensional MOFs.

The structural features and physicochemical properties of POFs are determined by the intrinsic nature of their precursors, such as organic structural units or organic ligands, and can thus be tuned through rational precursor selection. Furthermore, their pore structure and size are closely related to the linkage of the building blocks, which are adjusted via varying synthetic strategies and optimizing corresponding process parameters. Accordingly, the controllable synthesis methods of POFs will be reviewed in the following section.

SYNTHESIS OF POFS

In 1995, Yaghi *et al.*[3] synthesized a Co-based two-dimensional coordination polymer using trimesic acid (BTC) as the organic ligand by a solvothermal method, and formally proposed the concept of MOFs for the first time, opening the beginning of a new era for the synthesis of crystalline POFs. In 1999, the same group employed terephthalic acid (BDC) as the organic ligand to prepare the first permanently stable MOFs (named MOF-5) via the same solvothermal route, which marked a new milestone in research on stable POFs[36]. In 2005, they reported the first two-dimensional COFs constructed from six-membered macrocycles linked by borate ester rings, again using this synthetic method[4]. Since then, numerous synthetic strategies, including solvothermal/hydrothermal[37-39], mechanochemical[40-42], microwave- assisted[43-46], ionothermal[47-50], sonochemical[51-54], electrochemical methods[55-58], have been developed for the preparation of POFs with well-defined crystalline structures, high specific surface area, excellent structural stability and uniform pore size and distribution. Herein, these synthesis methods are briefly introduced in the following section.

(1) Solvothermal/hydrothermal method: Precursors are dissolved in an organic solvent or deionized water to form a uniform solution, which is then transferred into a well-closed container for chemical reaction under high temperature and pressure to produce target products[59,60]. The physicochemical properties of the resulting products are closely related to synthesis parameters such as reaction time, temperature, pressure, solution pH and surfactant addition. Although the solvothermal/hydrothermal method is suitable for the synthesis of most POFs, it still has some disadvantages: the solvothermal approach suffers from high cost,

complicated operation and potential safety hazards, while the hydrothermal method is restricted by relatively fixed reaction conditions.

(2) Mechanochemical method: Mechanical forces generated from grinding, squeezing, shearing and friction are used to drive low-temperature solid-phase chemical reaction for the preparation of target products under solvent-free or low-solvent conditions[61]. As compared to the solvothermal/hydrothermal method, this approach is conducive to reducing the particle diameter of target products and improving their physicochemical properties[62]. However, the quality of target products may be affected by by-products. Therefore, to realize the controllable synthesis of target products, it is critical to understand the distribution of applied forces under mechanical shock and reveal the relationship between applied forces and the chemical reaction of precursors.

(3) Microwave-assisted method: Based on the rapid heating effect of microwaves and the activization of polar substances, Gedye *et al.*[63] first utilized microwave-assisted synthesis to accelerate organic chemical reactions and synthesize seven different organic products in 1986. Since then, this method has been utilized to the preparation of numerous materials. In addition, microwave as an energy source is combined with other synthetic methods for materials preparation. Owing to its rapid heating and high thermal utilization efficiency, this method has been attracted increasing attention in the preparation of POFs, but it is still in the early stage. Many challenges, including limited product variety, uneven heating and thermal runaway, need to be addressed to promote its large-scale application.

(4) Ionothermal method: Ionic liquids are used as reaction solvents and structure-directing agents to synthesize target products with specific geometric structures under ambient conditions[64]. As compared to traditional solvothermal/hydrothermal method, this method exhibits four distinct advantages: moderate reaction conditions, rapid reaction, high product quality and low organic solvent consumption[65]. Moreover, this method is also integrated with other synthetic methods. Although it shows many advantages and has great potential for POFs preparation, its large-scale application is hindered by the high cost of ionic liquids.

(5) Sonochemical method: Owing to its unique acoustic cavitation effect, this method has been widely used for materials synthesis[66]. In this approach, ultrasonic waves produced by ultrasonic generators induce solution flow, leading to cavitation formation and nonuniform ultrasonic distribution in the solution. Bubbles in the rarefaction region of ultrasonic waves absorb surrounding dissolved gas and expand, whereas cavitation bubbles in the compression region rapidly collapse and burst, generating numerous microbubbles. The growth and collapse of these microbubbles produce strong shockwaves and create local extreme conditions, such as ultrahigh local temperature and pressure, which facilitate the nucleation and growth of target products[67]. This method offers advantages including fast reaction rates, low operating temperature, low energy consumption and nontoxicity, but its product purity and yield still need to be improved due to unexpected side reactions. Moreover, the industrial application of this method is limited by the scale of ultrasonic generators.

(6) Electrochemical method: According to different applied signal sources, this method is classified into cyclic voltammetry (CV), potentiostatic, galvanostatic, impulse and electrophoretic deposition[68]. In the CV method, target products are prepared by recording the oxidation or reduction current of precursors within a specific potential window[69]. Precursors are oxidized when scanning from low potential to high and reduced in the reverse direction. This method has three notable advantages: well-defined onset potential, controllable nucleation and growth process and suitability for the synthesis of multivalent materials[70]. In the potentiostatic deposition method, the response current at a constant potential is used to prepare target products, which includes underpotential and overpotential deposition. The rate of underpotential deposition

is correlated to interaction between the deposited target products and the substrates, whereas overpotential deposition is governed by an ion-diffusion-controlled nucleation process. Therefore, the structure and properties of target products prepared by potentiostatic deposition are related to the applied potential and ion species in the electrolyte[71]. Analogous to potentiostatic deposition, galvanostatic deposition uses a constant current to prepare target products. The difference is that the deposition reaction initiates after the charging of the electric double-layer in galvanostatic deposition[72]. In the pulsed deposition method, electrochemical pulses derived from periodically alternating applied potential are used to prepare target products. Target ions diffuse from the bulk electrolyte to the electric double-layer region at open-circuit potential and are then uniformly deposited on the substrate surface to form the target products at applied potential[73]. Unlike other electrochemical methods, electrophoretic deposition relies on electrostatic interaction between charged colloidal particle and substrate to fabricate target products, with the unique advantage that electrophoretic deposition is performed in poorly conductive electrolytes[74]. Owing to its diverse deposition modes, mild reaction conditions, fast reaction rates, nontoxicity and high product selectivity, electrochemical method has received extensive attention in the preparation of POFs.

In brief, solvothermal/hydrothermal methods are the most mature methods but are limited by high reaction pressure, long reaction time and the use of toxic organic solvents. The other five synthetic methods exhibit remarkable advantages, such as fast reaction rates, simple procedures, high efficiency, non-toxic solvents, low operating temperature and pressure, but they are restricted by requirements for specialized equipment, high cost and uncontrollable reaction conditions. Consequently, it is important to develop low-cost, green, rapid and general synthetic methods to achieve the large-scale and controllable synthesis of POFs.

POFS-BASED ELECTROCHEMICAL SENSORS

To mitigate the global food crisis exacerbated by population growth, OPs are widely used to improve food production and maintain quality. However, their overuse has given rise to serious food safety issues[72]. Benefiting from their unique structural features such as large specific surface area, tunable pore shape and size, high thermal/chemical stability and versatile multifunctionality, numerous POFs have been used for the adsorption and removal of OPs from foods[75-78]. It is precisely these distinctive structural properties that enable POFs-based materials to provide abundant catalytic active sites for catalyzing various electrochemical reactions such as oxygen reduction/evolution, hydrogen evolution, water splitting and carbon dioxide reduction reaction[79,80]. Consequently, their catalytic activity toward the electrochemical transformation of OPs has attracted much attention in the field of OPs electrochemical detection. Accordingly, POFs-based non-enzymatic electrochemical sensors have been constructed for detecting OPs in foods. In addition, POFs have also been employed as supporting platforms to immobilize bio-enzymes for the preparation of enzymatic electrochemical sensors for the determination of OPs[10,25]. Thanks to the continuous efforts of researchers, a large number of POFs-based electrochemical sensors have been developed and applied for the detection of OPs in foods. The following sections will focus on the research progress in the preparation and electrochemical detection performance of both non-enzymatic and enzymatic POFs-based electrochemical sensors.

Non-enzymatic electrochemical sensors

The detection performance of non-enzymatic electrochemical sensors (NEESs) for OPs is dependent to the catalytic activity of their electrochemical active materials, which are directly employed to modify conductive electrodes such as glassy carbon electrodes (GCE), carbon paper (CP), indium tin oxide (ITO), gold electrodes (AuE) and screen-printed electrodes (SPEs). The constructed sensors based on modified electrode are then immersed in electrolyte to detect the electrochemical response signals (i.e., current, potential and resistance) of OPs under specified measurement conditions. The linear relationship between the electrochemical response signals of OPs and their concentrations is employed to evaluate the key

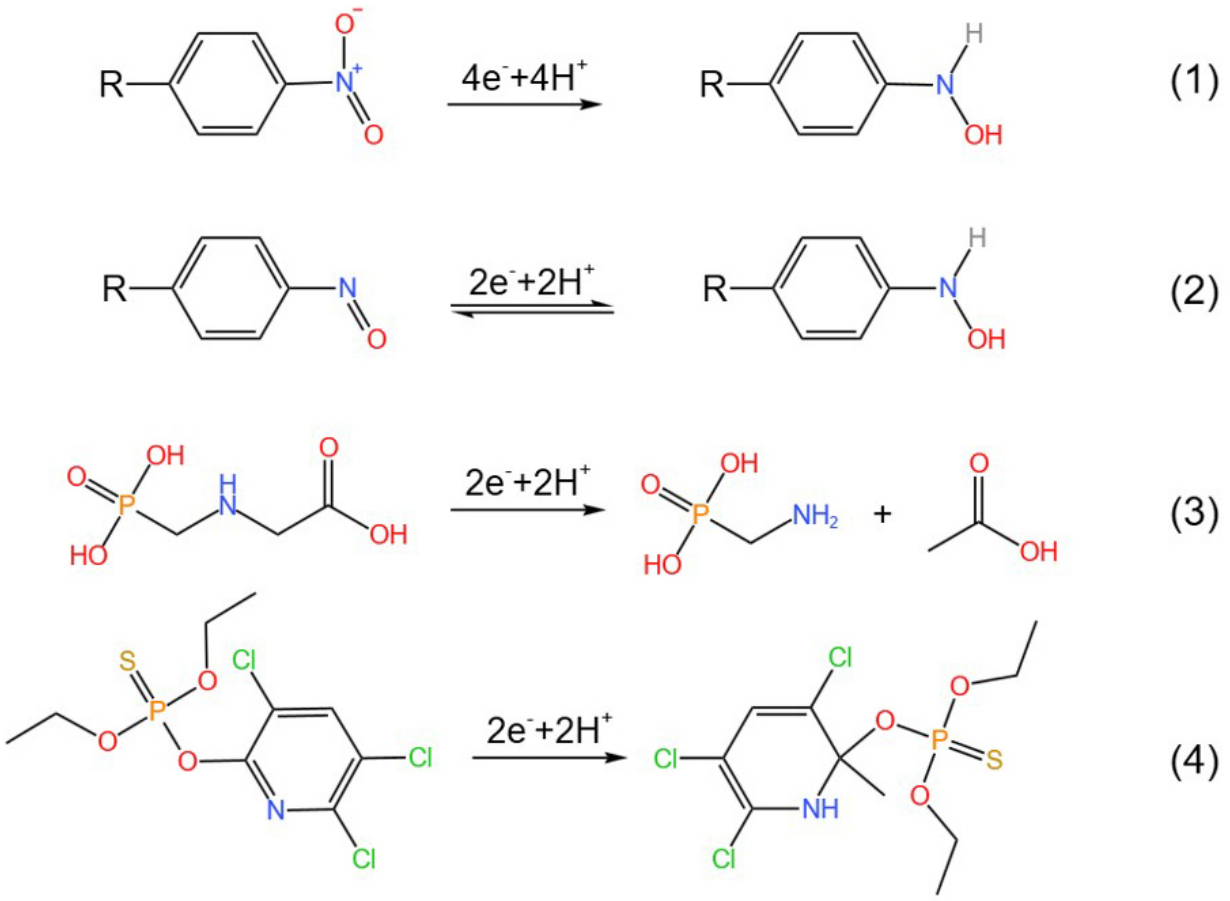

Figure 1. The electrochemical transformation mechanism of several typical OPs. OP: Organophosphorus pesticide.

electrochemical detection performance indicators [i.e., linear concentration range (LCR), sensitivity and LOD] of sensors for OPs. These detectable electrochemical response signals are originated from the electrochemical reaction of OPs occurred at the modified electrode surface of sensors. Owing to their different active functional groups, different OPs undergo electrochemical transformation via distinct reaction pathways. As shown in Figure 1, for OPs with nitro groups such as methyl parathion, parathion and paraoxon, their nitro groups are irreversibly transformed into hydroxylamine groups through a four-electron/proton pathway [Equation 1], while their nitroso groups are reversibly conversed into hydroxylamine groups through a two-electron/proton pathway [Equation 2][81]. Unlike nitro-containing OPs, glyphosate is cleaved at C-N bond via a two electron/proton pathway to yield (aminomethyl) phosphonic acid and acetic acid [Equation 3], and the pyridine ring of chlorpyrifos is reduced via a two electron/proton hydrogenation reaction [Equation 4][82]. Owing to their excellent catalytic activity for the electrochemical transformation of OPs, POFs have been widely applied to construct NEESs. Therefore, in the following section, their preparation and electrochemical detection performances for OPs will be emphatically discussed.

COFs-based sensors

In contrast to most common electrochemical reactions, such as such as oxygen reduction/evolution, hydrogen evolution and water splitting[79,80], the electrochemical reaction for the detection of OPs requires a large number of active metal centers in electrocatalysts to stabilize the reaction intermediates. However, most COFs lack metal ions in their native crystal structures, making them difficult to directly construct NEESs for the detection of OPs in food matrices. On the other hand, benefiting from their large specific surface area,

high porosity and excellent chemical/thermal stability derived from the strong covalent bonds between organic structural units, COFs are widely used for the physical adsorption and removal of pesticides residues from the environment[83]. Based on these characteristics, COFs are commonly integrated with enzyme-like electroactive materials to construct NEESs for OPs detection. For example, Zhang *et al.*[84] combined COFs with phosphatase-like CeO_2 to prepare NEESs, which achieved ultrahigh sensitivity and selectivity detection of methyl parathion. These performances originate from the ability of CeO_2 to cleave the P=O bonds of methyl parathion, producing form electroactive p-nitrophenol for electrochemical detection. In their work, spherical COFs were synthesized via solvothermal methods by dissolving 1,3,5-tris(4-aminophenyl) benzene and 2,5-dimethoxyterephaldehyde in mixed solution of 1, 4-dioxane, n-butanol and methanol. The as-prepared COFs were then sequentially modified with valine and CeO_2 to form a core-sell CeO_2-COFs composite, which was finally drop-coated on GCE surface for methyl parathion detection in grapes and tap water, as illustrated in Figure 2A. Under optimal reaction conditions (the solution pH value of 7 and incubation time of 5 min)[84], the fabricated sensors exhibited excellent electrochemical activity, anti-interference ability, reproducibility and stability for methyl parathion detection. which were attributed to the synergistic interaction between COFs and CeO_2. Square wave voltammetry (SWV) measurements revealed a linear relation between the peak current of the sensors and methyl parathion concentration, over a LCR of 34-7.6 × 10^4 nM, and the calculated LOD for methyl parathion was 11 nM. The recoveries of methyl parathion in grapes and tap water samples ranged from 97.46% and 111.10%. This work demonstrates that introducing electroactive inorganic materials to enhance the interaction between OPs and COFs is an effective strategy for constructing high-performance COFs-based NEESs for OPs detection.

MOFs-based sensors

Due to their abundant metal active centers, MOFs have attracted considerable attention for developing high-performance electrode materials for NEESs. In the following section, the application of both monometallic MOFs (such as Zr-, Cu-, Ni-, Fe- and rare earth metal)[85-89] and bimetallic MOFs (such as Zn-Cu, Mn-Fe and Co-Mn)[90-92] for the detection of OPs is discussed in detail.

Zr-MOFs

Because the Zr-O groups of Zr-MOFs can specially interact with the P=O/S groups of OPs to form stable Zr-O-P bonds[93], Zr-MOFs have been widely employed to construct NEESs for the detection of OPs. For instance, Gao *et al.*[85] deposited Zr-BDC MOFs and single-layer graphene oxide (GO) on the surface of GDE by co-electroreduction methods to assemble NEESs for methyl parathion detection. Under optimal detection conditions, SWV results revealed two linear relations between the sensors' peak current and methyl parathion concentration. One LCR was 1-50 ng mL^{-1} and the other was 50-3,000 ng mL^{-1}. The corresponding calculated LOD of the sensors for methyl parathion was 0.5 ng mL^{-1}, and the recovery rates of methyl parathion in cabbage samples were 95.3%-103.4%. In addition, Gokila *et al.*[94] utilized the synergistic effect between ZrO_2 nanoparticles (which provide active sites), Zr-MOFs (which provide additional active sites) and multi-walled carbon nanotubes (MWCNTs, which enhance conductivity) to prepare NEESs for multiple OPs detection [Figure 2B]. Electrochemical impedance (EIS) results gave the calculated LODs of 1.11 nM for monocrotophos, 2.01 nM for glyphosate, 2.02 nM for malathion, 2.5 nM for dimethoate and 2.8 nM for chlorpyrifos, respectively. Similarly, single-wall carbon nanotubes (SWCNTs) have also been employed to enhance the detection performance of NEESs. Han *et al.*[95] modified GCE with SWCNT networks and Ui-66 for methyl parathion detection. Electrochemical analysis indicated that the sensors' peak current increased linearly with methyl parathion concentration over the LCR of 10-10^4 nM under optimized reaction conditions. The calculated LOD was 8.05 nM. Their distinguished electrochemical detection performance was attributed to the enhanced electron and ion transfer between the sensors and OPs, induced by the formation of conductive carbon networks.

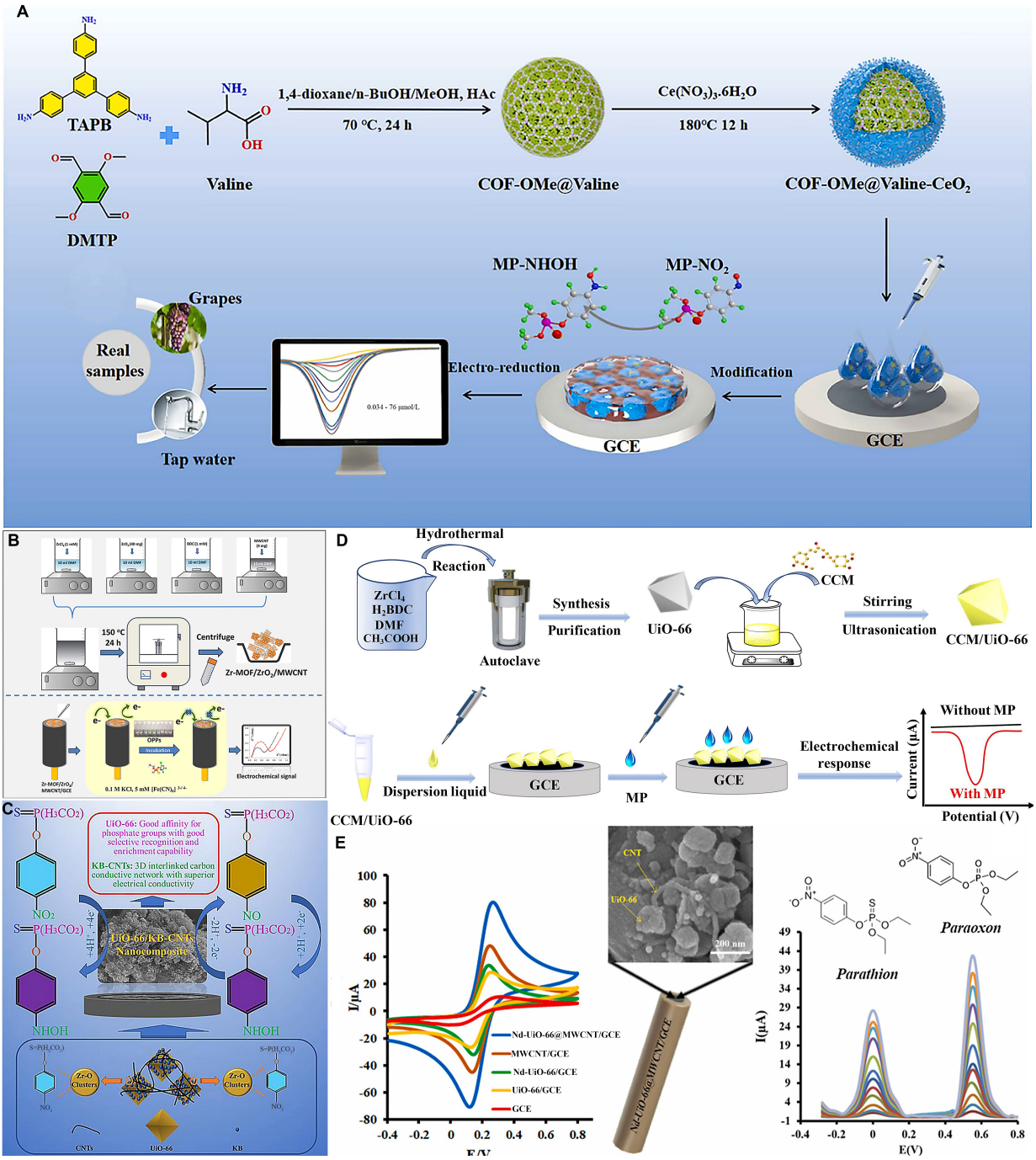

Figure 2. (A)The preparation of CeO_2-COFs (Reproduced with permission[84]. Copyright 2024, Elsevier), and (B) Zr-MOFs-ZrO_2-MWCNTs (Reproduced with permission[94]. Copyright 2024, Academic Press), NEESs; (C) The detection mechanism of UiO-66-KB-CNTs for methyl parathion (Reproduced with permission[96]. Copyright 2023, Elsevier); (D) The preparation of UiO-66-curcumin NEESs (Reproduced with permission[22]. Copyright 2023, Elsevier); (E) The simultaneous detection of Nd-UiO-66-MWCNTs for parathion and paraoxon (Reproduced with permission[97]. Copyright 2022, Pergamon). TAPB: 1,3,5-tris(4-aminophenyl)benzene; DMTP: 2,5-dimethoxyterephaldehyde; COF: covalent organic framework; GCE: glassy carbon electrode; MOF: metal-organic framework; MWCNT: multi-walled carbon nanotube; NEES: non-enzymatic electrochemical sensor; UiO-66: zirconium 1,4-dicarboxybenzene metal-organic framework.

To further improve the electrochemical performance of Zr-MOFs-based NEESs for OPs detection, Guo *et al.*[96] synthesized zirconium 1,4-dicarboxybenzene metal-organic framework (UiO-66)-KB-CNTs composites using Ketjen black (KB)-carbon nanotubes as conductive additives to fabricate NEESs [Figure 2C].

Differential pulse voltammetry (DPV) results demonstrated two linear relations between sensors' peak current and methyl parathion concentration under optimized detection conditions. One LCR was 5-10^3 nM, and the other was 10^3-1.2 × 10^4 nM. The calculated LOD and limit of quantification (LOQ) were 1.53 and 5.1 nM, respectively. The sensors also exhibited outstanding electrochemical detection performance, including considerable reproducibility, stability, selectivity and satisfactory recovery rates for methyl parathion in real samples, which was attributed to the fast electron transfer between octahedral UiO-66 particles and the three-dimensionally interconnected network formed by KB and CNTs. Furthermore, Duan *et al.*[22] prepared UiO-66-curcumin composites by one-pot hydrothermal method and modified GCE with as-prepared materials, as illustrated in Figure 2D. Electrochemical analysis indicated a linear relationship between methyl parathion concentration and the sensors' peak current over the LCR of 20-2.0 × 10^4 ng mL^{-1}, with a corresponding calculated LOD of 0.98 ng mL^{-1}. The methyl parathion recoveries achieved with the sensors were 95.00%-111.73% in tomato, 95.70%-114.80% in cucumber and 98.69%-111.81% in peach samples, respectively.

The rare earth elements have also been introduced to improve the electrochemical performance of Zr-MOFs, Khoshsafar *et al.*[97] first prepared Nd-doped Ui-66 by solvothermal methods, then integrated the as-prepared materials with MWCNTs to modify GCE, achieving simultaneous detection of parathion and paraoxon, as shown in Figure 2E. Electrochemical analysis confirmed that the sensors exhibited outstanding detection performance for parathion and paraoxon, including excellent electrocatalytic activity, stability, selectivity and repeatability, under optimized detection conditions. The sensors' peak current was directly proportional to the concentration of the target OPs, with the LCRs of 0.7-100 nM for parathion and 1-120 nM for paraoxon, and corresponding LODs of 0.04 nM and 0.07 nM, respectively. The sensors also achieved satisfactory recoveries for parathion and paraoxon in tomato, spinach, cabbage and water samples.

In short, Zr-MOFs are regarded as one of the most promising electrode materials for constructing of NEESs for the detection of OPs. The introduction of other electroactive materials, conductive additives, signal amplification agents and heterogeneous atoms can further improve the detection performance of Zr-MOFs-based NEESs, making their LOD to reach the nanomole level.

Cu-MOFs

It is reported that the Cu ion centers of Cu-MOFs can specially interact with the amine, carboxylate and phosphate group of glyphosates to form a quinary equatorial plane[98]. As a result, numerous efforts have been devoted to exploring the electrochemical detection performance of Cu-MOFs for glyphosate. As shown in Figure 3A, the earliest study using Cu-MOFs as electrode materials for non-enzymatic electrochemical detection of glyphosate was conducted by Cao *et al.*[86]. At an incubation potential of 0.1 V and an incubation time of 150 s, Cu-BTC MOFs modified ITO electrodes were found to show excellent electrochemical activity, stability, reproducibility and selectivity. Electrochemical analysis indicated two linear relationships between glyphosate concentration and the sensors' peak current under optimal detection conditions. The linear ranges were 10^{-3}-1.0 nM and 1.0-10^4 nM, and the calculated LOD was 1.4 × 10^{-4} nM. On the one hand, leveraging the synergistic interaction between the π-conjugated structure of porphyrin and the ultrahigh conductivity of Au nanoparticles (NPs)[99], Jiang *et al.*[100] coated Cu-TCPP (tetra(4-carboxyphenyl)porphine) MOFs on CP decorated with Au NPs to fabricate NEESs for detecting glyphosate [Figure 3B]. The as-prepared sensors displayed considerable electrochemical activity, acceptable reproducibility, excellent selectivity and good stability, with a LCR of 20-1.2 × 10^5 nM and a LOD of 30 nM. For real sample analysis, the recoveries of glyphosate in soybean, carrot, wheat, and water samples were 97.5%-110.7%. On the other hand, taking advantage of the large specific surface area and delocalized π-electron system of carbon nanofibers (CNFs)[101], Dey *et al.*[102] anchored flower-like Cu-PZDA MOFs on the surface of CNFs and modified GCE to prepare NEESs for the detection of glyphosate. DPV analysis revealed that the sensors'

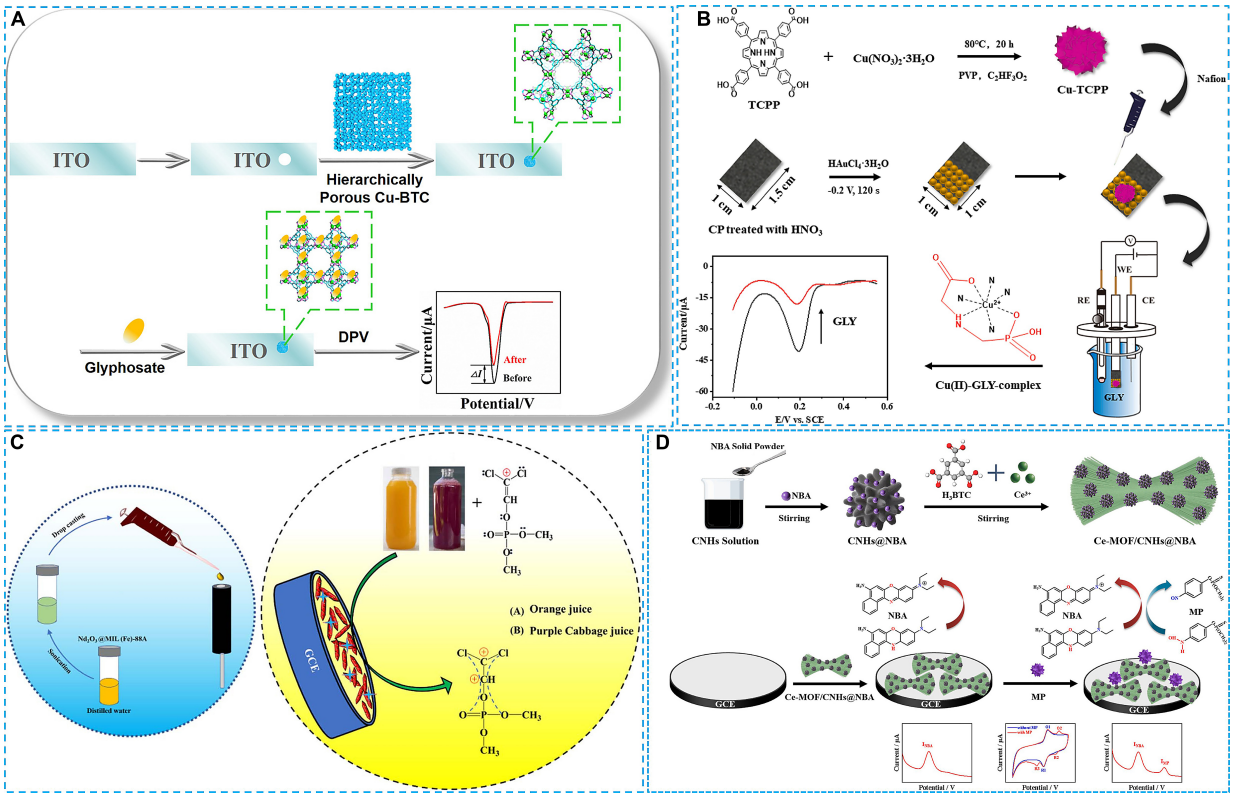

Figure 3. (A) The preparation of Cu-BTC MOFs (Reproduced with permission[86]. Copyright 2019, Elsevier), (B) Cu-TCPP MOFs (Reproduced with permission[100]. Copyright 2022, Elsevier), (C) Nd_2O_3-Fe MOFs (Reproduced with permission[105]. Copyright 2023, Royal Society of Chemistry), (D) Ce-MOFs (Reproduced with permission[106]. Copyright 2026, Elsevier), NEESs. ITO: Indium tin oxide; DPV: differential pulse voltammetry; TCPP: tetra(4-carboxyphenyl)porphine; PVP: polyvinylpyrrolidone; GLY: glyphosate; GCE: glassy carbon electrode; BTC: trimesic acid; NBA: nile blue A; MP: methyl parathion; MOF: metal-organic framework; NEES: non-enzymatic electrochemical sensor; H_3BTC: benzenemalic acid.

peak current increased with increasing glyphosate concentration, with a LCR of 10 - 500 nM, a LOD of 3.12 nM, LOQ of 10.18 nM, sensitivity of 173.88 μA μM^{-1} cm^{-2} respectively. The sensors exhibited high stability, excellent reproducibility and considerable recovery rates for glyphosate in beetroot juice and lettuce extract samples. Their remarkable electrochemical performance was attributed to accelerated electron transfer in the sensors.

In short, sensors based on Cu-MOFs exhibit outstanding electrochemical performance for the detection of glyphosate, with the lowest reported LOD reaching as low as 5.17×10^{-3} nM. Various strategies, including modification of organic ligand and introduction of conductive materials, have been proven effective for improving the electrochemical performance Cu-MOFs-based sensors for glyphosate detection[100,102]. However, the specific recognition of glyphosate by Cu-MOFs hinders their application in the detection of other OPs. Therefore, it is important to develop novel Cu-MOFs for the detection of other OPs.

Ni- MOFs

Analogous to the Cu ion centers in Cu-MOFs, the Ni ion centers in Ni-MOFs can also specifically bind to glyphosate. Accordingly, Patel *et al.*[87] reported that nickel nitrate hexahydrate and 1,4-benzene dicarboxylic acid were dissolved in a mixed solution of N, N-dimethylformamide and ethylene glycol, and two-dimensional tabular Ni-MOFs synthesized by the solvothermal methods. The vibrational modes of functional groups and the type, concentration and valence state of elements on the surface of Ni-MOFs were characterized by multiple analytical methods. CV results indicated that the peak current of Ni-MOFs

decorated SPE in electrolyte without glyphosate were much high than those of the electrode with glyphosate. This indicates that glyphosate can inhibit electron transfer on modified electrode by occupying its electrochemical active sites. Electrochemical analysis indicated that the sensors' peak current decreased with increasing glyphosate concentration. The LCR was 166-666 nM, and the corresponding LOD was calculated to be 0.0113 nM. Based on the standard addition recovery method, the recovery of glyphosate was 96.50%-106.66% in tap water and 90%-115% in soil samples, respectively. The findings show that NEESs based on Ni-MOFs have promising practical application prospects for glyphosate detection.

Fe-MOFs

In addition to Zr, Cu and Ni ions, Fe ions have also been used as metal nodes for the fabrication of MOFs, and a variety of Fe-MOFs have been applied to construct NEESs for the detection of OPs, including chlorpyrifos and dichlorvos. For instance, using iron nitrate hexahydrate as the metal precursor, Dey *et al.*[88] first grew sponge-like Fe-MOFs on the surface of CNFs using one-pot solvothermal methods, and then modified GCE to construct NEESs for detecting chlorpyrifos. Electrochemical analysis demonstrated that the sensors exhibited distinguished electrochemical detection performance, inculding high electrocatalytic activity, stability and selectivity for the detection of chlorpyrifos under optimized reaction conditions. The electrochemical results also indicated a linear relationship between chlorpyrifos concentration and the sensors' peak current. The LCR was 10^3-1.5 × 10^5 nM, with a LOD of 15.1 nM, LOQ of 50.3 nM and sensitivity of 40.47 μA μM^{-1} cm^{-2}. The recoveries of chlorpyrifos in tomato and cucumber juice were 98.91%-99.26% and 98.05%-99.58%, respectively. Their outstanding detection performance was derived from the large surface area and high porosity of the sponge-like Fe-MOFs. Since rare earth metal oxides can provide abundant active sites for the adsorption of bioactive molecules in solution[103,104], Narayanan *et al.*[105] immobilized Nd_2O_3 clusters on the surface of rod-like Fe-MOFs and used the composites to modify GCE to fabricate NEESs for detecting dichlorvos [Figure 3C]. The sensors displayed excellent electrochemical performance for the detection of dichlorvos, with a LCR of 1 to 250 nM, LOD of 0.92 nM and sensitivity of 4.42 mA nM^{-1}. The recoveries of dichlorvos were 96%-97% for purple cabbage and 99.5-103.4% for orange juice, respectively. The excellent detection performance is likely related to the electrostatic interaction between the positively charged dichlorvos molecules and the π-π electrons of the Nd_2O_3-Fe-MOFs composites. Unlike Cu- and Ni-MOFs that can only specifically detect a single type of OPs[87,98], these NEESs based on Fe-MOFs are used to detect multiple types of OPs. Therefore, the design and fabrication of Fe-MOFs for the simultaneous detection of multiple OPs is of great significance.

Rare earth metal-MOFs

To develop novel monometallic MOFs for the detection of OPs, Yassin *et al.*[89] first synthesized micron-sized rod-shaped Sm-BDC MOFs via hydrothermal methods, by dissolving samarium acetate hydrated and terephthalic acid in deionized water. The Sm-BDC MOFs were then incorporated with graphitic carbon nitride (g-C_3N_4) and cadmium sulfide (CdS) to modify GCE. Electrochemical analysis revealed that the sensors displayed ultrahigh electrocatalytic activity, excellent selectivity, outstanding sensitivity, good repeatability and remarkable stability for the detection of malathion. The electrochemical results also showed the peak current increased linearly with increasing the malathion concentration, over the range of 30 and 150 nM, with a LOD of 7.4 nM and a sensitivity of 25 μA μM^{-1}. The recovery of malathion in cabbage samples was 86.4-107.6%. Their outstanding detection performance was attributed to the synergistic interaction between the conductivity of g-C_3N_4, the active sites of CdS and the specific surface area of Sm-BDC. Furthermore, Tao *et al.*[106] prepared Ce-MOFs-(carbon anohorns, CNHs)-(nile blue A, NBA) composites by two-step liquid phase synthesis, and used as-prepared composites to modify GCE for constructing NEESs for methyl parathion detection, as illustrated in Figure 3D. Electrochemical analysis showed that the sensors' current exhibited a good linear relationship with methyl parathion concentration in the range of 0.05-50 μg mL^{-1}, and the corresponding LOD was calculated to be 18.8 ng mL^{-1}. The as-prepared electrochemical sensors

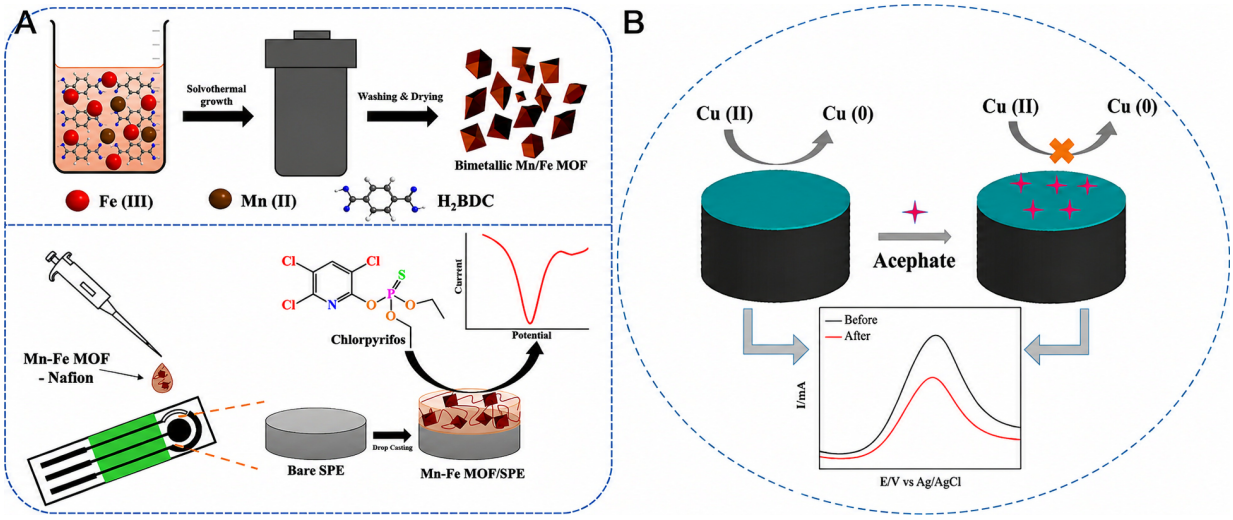

Figure 4. (A) The preparation of Mn-Fe MOFs NEESs (Reproduced with permission[90]. Copyright 2022, Elsevier); (B) the detection mechanism of Zn-Cu MOFs for acephate (Reproduced with permission[91]. Copyright 2023, Elsevier). MOF: Metal-organic framework; SPE: screen-printed electrode; NEES: non-enzymatic electrochemical sensor.

also displayed excellent selectivity, remarkable reproductivity and good stability. The recoveries of methyl parathion in bok choy, cucumber and cabbage samples were 90.1%-109.5%, which were in accordance with the results obtained by high performance liquid chromatography. Their distinguished electrochemical performance was attributed to the synergistic interaction between the multivalent redox activity of Ce^{3+}/Ce^{4+}, the good electrical conductivity of carbon nanohorns and the high specific surface area of Ce-MOFs. The fabrication of these novel NEESs provides a new option for the detection of OPs.

Bimetallic MOFs

It is reported that the electrochemical activity, stability and selectivity of bimetallic MOFs are far superior to those of monometallic MOFs, owing to the synergistic effect between their heterogeneous metal ion centers[107]. Accordingly, numerous efforts have been devoted to the development of bimetallic MOFs-based NEESs for OPs detection. For instance, Janjani *et al.*[90] decorated SPE with bimetallic Mn-Fe MOFs, which possessed abundant unsaturated coordination defects, high porosity and distortion structures, to construct NEESs for chlorpyrifos detection, as shown in Figure 4A. SWV analysis indicated that the sensors' peak current increased with increasing chlorpyrifos concentration, with a LCR of 1-100 nM. The corresponding LOD was calculated to be 0.85 nM. Their remarkable detection performance was ascribed to the synergistic interaction between Mn and Fe metal centers. Subsequently, they modified GCE using Zn-Cu MOFs as the sensing agent and activated charcoal as the conductive additive to detect acephate[91]. Due to the inhibitory effect of acephate on the sensors [Figure 4B], DPV analysis confirmed that the sensors' peak current decreased with increasing acephate concentration under optimal reaction conditions. The LCR was 0.1-10 nM, with a LOD of 3.3×10^{-3} nM. The recoveries for acephate in cucumber and tomato juice were 97%-107% and 95.2%-103%, respectively. In addition, they also employed Co-Mn MOFs to modify SPE for detecting dichlorvos[92]. a linear relationship between the concentration of dichlorvos and the sensors' peak current was observed in the range of 1-12 nM, with a LOD of 0.645 nM. It is concluded that bimetallic MOFs NEESs exhibit outstanding detection capability for OPs.

Table 1 systematically summarizes the LCR, LOD, LQD, sensitivity, reproducibility, anti-interference capability, repeatability and recovery rate in real samples of POFs-based NEESs. According to Table 1, these sensors exhibit broad LCR ranging from nanomolar to micromolar levels, with extremely low LOD reaching the picomolar level, good repeatability and reproductivity with the relative standard derivations (RSD) of as

low as 5%, and remarkable recovery rate for OPs in real samples ranging from 90% to 120%, as well as high anti-interference ability against common interfering inorganic ions and internal interfering between OPs. Although the reported POFs-based NEESs have displayed excellent detection performance for OPs, their practical applications have not been realized yet, mainly due to insufficient storage stability; most sensors retain less than 90% of their initial catalytic activity after storage under ambient conditions. To realize the practical application of POFs-based NEESs, strategies including the introduction of conductive additives, transition metal oxides and heterogeneous doping have been widely adopted to further optimize their detection performance. It is worth noting that the detection performance of POFs-based NEESs is closely related to the type of metal ions (or clusters) and organic structural units of POFs. For example, although NEESs based on Zr-MOFs with terephthalic acid as organic structural unit have been mainly used for the detection of methyl parathion[95,96], replacing terephthalic acid with 4,4'-Biphenyl diacid to construct UiO-67 enables the corresponding sensors to detect profenofos[108]. In addition, when Nd ions are introduced into a Zr-MOFs matrix, the resulting Nd-doped Zr-MOFs-based sensors can be applied for the detection of parathion and paraoxon. Meanwhile, Cu-MOFs-based NEESs are predominantly employed for the detection of glyphosate, owing to the specific coordination interaction between Cu ions and glyphosate. Therefore, the rational design and synthesis of POFs are conducive to achieving highly selective electrochemical detection toward target OPs.

Enzymatic electrochemical sensors

As everyone knows, AChE can catalyze the hydrolysis of acetylthiocholine (ATCh) to produce thiocholine (TCh). Under an applied potential, the electrochemical oxidization of TCh generates a detectable response signal, owing to the electrochemical reduction activity of its sulfhydryl groups[110]. Unfortunately, the hydrolysis of ATCh is reduced by the inhibition of AChE's electrocatalytic activity originating from OPs, thereby decreasing the production of TCh and causing a reduction in the electrochemical oxidization response signal of TCh. Based on this electrochemical reaction mechanism, cholinesterase is used as a recognition element to construct enzymatic electrochemical sensors (EESs) for the detection of OPs[111]. In addition, the preparation of EESs is almost identical to that of non-enzymatic electrochemical sensor, with the only difference being that cholinesterase is immobilized on the modified electrode in the enzymatic configurations. Nonetheless, the electrochemical performance evaluation metrics and technologies of EESs are consistent with those for NEESs. Due to their outstanding physicochemical properties, POFs, as one of the most ideal support materials for biological enzymes, have been attracted significant attention in the field of EESs for OPs detection. In this section, the preparation and electrochemical detection performance of EESs for OPs will be discussed.

COFs-based sensors

COFs-based materials possess enormous potential for the immobilization of biological enzymes[7]. In the traditional "turn off" EESs, TCh and $[Fe(CN)_6]^{3-}$ are commonly employed as response signal producers, which always causes insufficient selectivity and repeatability[112]. In order to solve this problem, Wang *et al*[23] anchored AChE on the surface of GCE decorated with COF-NFs to construct a low-potential "turn-on" EES with $[Ru(bpy)_3]^{2+}$ as the response signal producer, as illustrated in Figure 5A. The electrochemical detection performance and stability for dichlorvos of the as-fabricated "turn-on" sensor were comparable to those of the "turn off" sensors, while their selectivity and repeatability were significantly higher than those of "turn off" sensors. Additionally, Wang *et al.*[113] prepared core-shell COFs-MWCNTs composites to modify GCE, and then immobilized AChE on the modified electrode for malathion detection. Under optimal detection conditions, electrochemical results demonstrated that the oxidation current of ATCh chloride was directly proportional to its concentration over the LCR of 1-10^4 nM, and the corresponding LOD was calculated to be 0.5 nM. The recovery rates for malathion in tap water and spinach samples were 96.0%-101.6% and 98.0%-105.0%, respectively.

Table 1. The detection performance of NEESs for OPs

Sensors	Detection performance	Ref.
COF-Valine-CeO_2/GCE	LCR for methyl parathion: 34-7.6 × 10^4 nM; LOD: 11 nM; Stability (15 days): > 95% of initial activity; Repeatability (7 times): relative standard derivations (RSD) of 4.02%; Anti-interference capability: OPs containing P=S groups, inorganic ions; Recovery rate in real samples: 97.46%-111.10%	[84]
Curcumin-UiO-66/GCE	LCR for methyl parathion: 20-2 × 10^4 ng mL^{-1}; LOD: 0.98 ng mL^{-1}; Stability (18 days): > 95% of initial activity; Repeatability (8 times): RSD of 5.8%; Reproducibility (5 electrodes): RSD of 2.9%; Anti-interference capability: carbofuran, malathion, chlorpyrifos, heptachlor epoxide, inorganic ions; Recovery rate in real samples: 95.00%-114.80%	[22]
Zr-BDC-rGO/GCE	LCR for methyl parathion: 1-3 × 10^3 ng mL^{-1}; LOD: 0.5 ng mL^{-1}; Stability (28 days, 4 °C): 92.1% of initial activity; Anti-interference capability: other electroactive nitrophenyl derivatives, inorganic ions; Recovery rate in real samples: 95.30%-103.40%	[85]
Zr-MOF-ZrO_2-MWCNT/GCE	LCR: 5-7 × 10^4 nM (malathion, chlorpyrifos, dimethoate and monocrotophos) and 5 -5 × 10^4 nM (glyphosate); LOD: 2.02 nM (malathion), 2.8 nM (chlorpyrifos), 2.5 nM (dimethoate), 1.11 nM (monocrotophos) and 4.21 nM (glyphosate); Stability (28 days): 86.8% of initial activity; Reproducibility (10 electrodes): RSD of 3.19%; Anti-interference capability: 2,4-dichlorophenoxyacetic acid, atrazine, carbendazim, thiophanate methyl; Recovery rate in real samples: 95.04%-99.30%	[94]
SCN-UiO-66/GCE	LCR for methyl parathion: 10-10^4 nM; LOD: 8.05 nM; Reproducibility (5 electrodes): RSD of 1.22%; Repeatability (5 times): RSD of 0.34%; Anti-interference capability: glucose, niclosamide, carbendazim, inorganic ions; Recovery rate in real samples: 98.28%-101.95%	[95]
UiO-66-KB-CNTs/GCE	LCR for methyl parathion: 5-1.2 × 10^4 nM; LOD: 1.53 nM; LOQ: 5.1 nM; Repeatability (5 times): RSD of 1.61%; Reproducibility (5 electrodes): RSD of 4.85%; Anti-interference capability: hydroquinone, paranitroaniline, isoproturon, pnitrophenol, carbendazim, catechol, inorganic ions; Recovery rate in real samples: 96.14%-102.93%	[96]
Nd-UiO-66-MWCNT/GCE	LCR: 0.7-100 nM (parathion) and 1-120 nM (paraoxon); LOD: 0.04 nM (parathion) and 0.07 nM (paraoxon); Stability (7 days): 85.1% (parathion) and 87.6% (paraoxon) of initial activity; Repeatability (5 times): RSD of 2.6% (parathion) and 2.2% (paraoxon); Anti-interference capability: carbaryl, fenamiphos, carbofuran, diazinon, inorganic ions; Recovery rate in real samples: 93.5%-105.3%	[97]
UiO-67-GO/AuE	LCR for profenofos: 10^4-5 × 10^5 nM; LOD: 90 nM; LOQ: 300 nM; Stability (45 days): 97.76% of initial activity; Reproducibility (3 electrodes): RSD of 1.75%; Repeatability (7 times): RSD of 0.5%; Anti-interference capability: thiamethoxam, carbendazim, imidacloprid, endosulfan, inorganic ions; Recovery rate in real samples: 98.82%-108.89%	[108]
Cu-BTC/ITO	LCR for glyphosate: 10^{-3}-10^4 nM; LOD: 1.4×10^{-4} nM; Stability (14 days, 4 °C): > 90% of initial activity; Repeatability (10 times): RSD of 4.1%; Anti-interference capability: trichlorfon, carbendazim, acetochlor, thiram, inorganic ions; Recovery rate in real samples: 98.0%-105.0%	[86]
Cu-TCPP-AuNPs/CP	LCR for glyphosate: 200-1.2 × 10^5 nM; LOD: 30 nM; Stability (14 days, 4 °C): 86.6% of initial activity; Reproducibility (6 electrodes): RSD of 2.5%; Anti-interference capability: dime thoate, (aminomethyl)phosphonic acid, acephasste, parathion, inorganic ions; Recovery rate in real samples: 97.5%-110.7%	[100]
Cu-PZDA-CNF/GCE	LCR for glyphosate: 10-2 × 10^5 nM; LOD: 3.12 nM; LOQ: 10.18 nM; Sensitivity: 173.88 μA $μM^{-1}$ cm^{-2}; Stability (45 days): 97.76% of initial activity; Reproducibility (5 electrodes): RSD of 1.34%; Repeatability (5 times): RSD of 2.56%; Anti-interference capability: fenitrothion, chlorpyrifos, malathion, dichlorvos, acetamiprid, carbendazim, inorganic ions; Recovery rate in real samples: 98.01%-101.83%	[102]
Ni-MOF/SPE	LCR for glyphosate: 166-666 nM; LOD: 0.0013 nM; Reproducibility (10 electrodes): RSD of 2.8%; Anti-interference capability: malathion, chlorpyrifos, dichlorvos, inorganic ions; Recovery rate in real samples: 90%-115%	[87]
Fe-PyDA-CNF/GCE	LCR for chlorpyrifos: 10^3-1.5 × 10^5 nM; LOD: 15.1 nM; LOQ: 50.3 nM; Sensitivity: 40.47 μA $μM^{-1}$ cm^{-2}; Stability (30 days, 4 °C): 98.45% of initial activity; Reproducibility (5 electrodes): RSD of 0.95%; Repeatability (10 times): RSD of 2.56%; Anti-interference capability: chlorophenol, chlorobenzene, carbamate, fenitrothion, acetamiprid, imidacloprid, inorganic ions; Recovery rate in real samples: 98.09%-99.58%	[88]
MIL-88B(Fe) MOF/SPE	LCR for malathion: 10^{-3} -10^3 nM; LOD: 7.92×10^{-4} nM; Sensitivity: 53.46 μA nM^{-1} cm^{-2}; Stability (10 days): > 95% of initial activity; Reproducibility (5 electrodes): RSD of 3.27%; Anti-interference capability: glucose, sucrose, dichlorvos, glyphosate, chlorpyrifos, inorganic ions; Recovery rate in real samples: 97.08%-104.90%	[109]
Nd_2O_3-MIL(Fe)-88A/GCE	LCR for dichlorvos: 1-250 nM; LOD: 0.92 nM; Sensitivity: 4.42 mA nM^{-1}; Repeatability (3 times): RSD of ≤ 2.5%; Anti-interference capability: methyl parathion, amitrole, deltamethrin, triazolone, inorganic ions; Recovery rate in real samples: 96%-103.4%	[105]
CdS-Sm-BDC-g-C_3N_4/GCE	LCR for malathion: 30-150 nM; LOD: 7.4 nM; Sensitivity: 25.03 μA $μM^{-1}$; Stability (45 days): 97.76% of initial activity; Reproducibility (11 electrodes): RSD of 1.44%; Repeatability (5 times): RSD of 4.3%; Anti-interference capability: inorganic ions; Recovery rate in real samples: 86.4-107.6%	[89]
Ce-MOFs-CNHs-NBA-GCE	LCR for methyl parathion: 0.05-50 μg mL^{-1}; LOD: 18.8μg mL^{-1}; LOQ: 62.7μg mL^{-1}; Sensitivity: 173.88 μA $μM^{-1}$ cm^{-2}; Stability (14 days): 86% of initial activity; Reproducibility (7 electrodes): RSD of 3.2%; Repeatability (3 times): RSD of 3.4%; Anti-interference capability: chloramphenicol, thiabendazole, ascorbic acid, fenitrothion, carbendazim, inorganic ions; Recovery rate in real samples: 90.1%-109.5%	[106]

MnFe-MOFs/SPE	LCR for chlorpyrifos: 1-100 nM; LOD: 0.852 nM; Sensitivity: 28.46 μA μM^{-1} cm^{-2}; Stability (45 days): 97.76% of initial activity; Reproducibility (5 electrodes): RSD of 3.48%; Repeatability (10 times): RSD of 2.56%; Anti-interference capability: glucose, sucrose, inorganic ions; Recovery rate in real samples: 99.14%-106.81%	[90]
ZnCu-MOFs/GCE	LCR for acephate: 0.1-10 nM; LOD: 3.3 × 10^{-3} nM; Stability (5 days, 20 °C): 97% of initial activity; Repeatability (5 times): RSD of 4%; Anti-interference capability: glyphosate, dichlorvos, chlorpyriphos, inorganic ions; Recovery rate in real samples: 95.2%-107%	[91]
CoMn-MOFs/SPE	LCR for dichlorvos: 1-10 nM; LOD: 0.645 nM; Anti-interference capability: chlorpyrifos, malathion, glyphosate, inorganic ions; Recovery rate in real samples: 90%-118%	[92]

NEES: Non-enzymatic electrochemical sensor; OP: organophosphorus pesticide; COF: covalent organic framework; GCE: glassy carbon electrode; LCR: linear concentration range; MOF: metal-organic framework; LOD: limit of detection; BDC: terephthalic acid; rGO: reduced graphene oxide; LOQ: limit of quantification; UiO-66-KB: CNT: carbon nanotube; MWCNT: multi-walled carbon nanotube; BTC: trimesic acid; ITO: indium tin oxide; SPE: screen-printed electrode; CP: carbon paper; CNH: carbon anohorn.

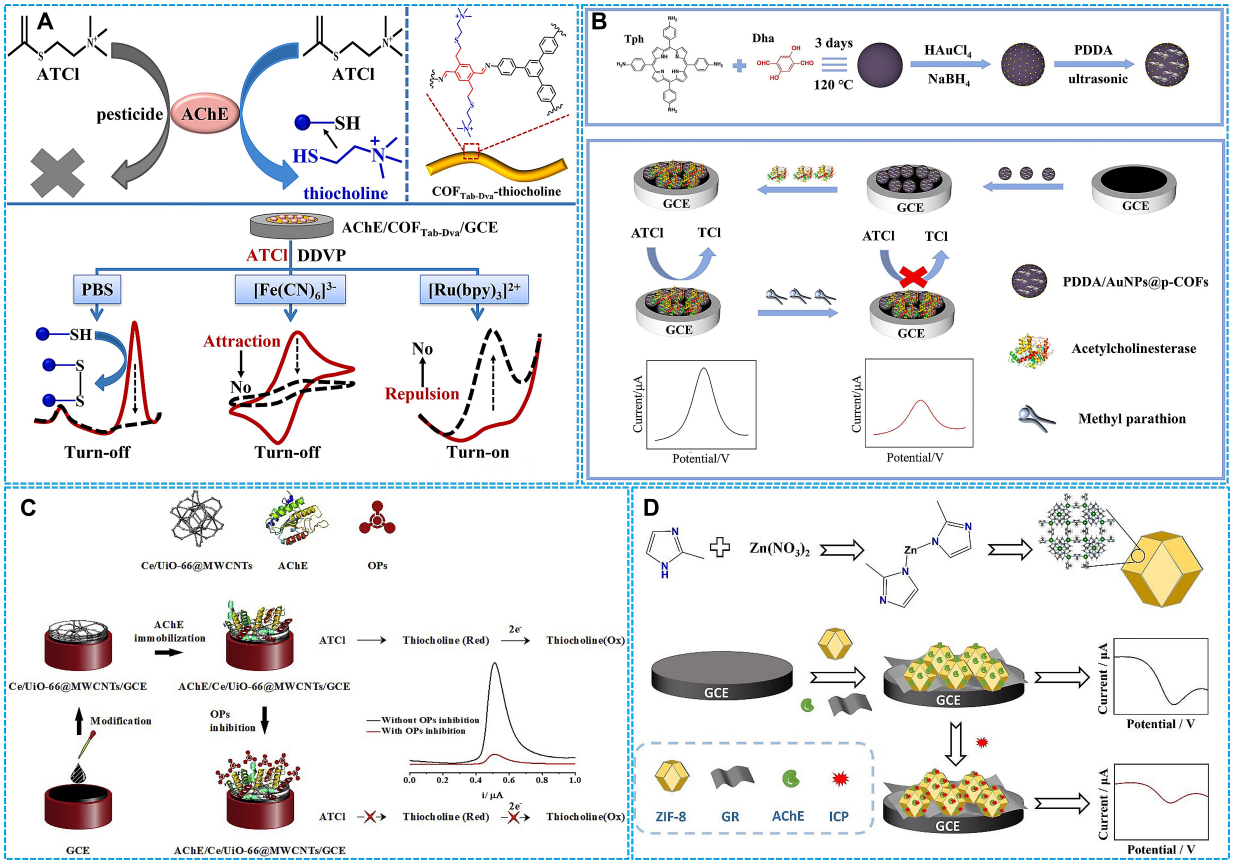

Figure 5. (A)The detection mechanism of "turn off" and "turn on" EESs (Reproduced with permission[23]. Copyright 2022, Elsevier), (B) the preparation of PDDA-AuNPs-COFs (Reproduced with permission[114]. Copyright 2024, Elsevier), (C) Ce-UiO-66-MWCNTs (Reproduced with permission[115]. Copyright 2019, Elsevier), (D) AChE-CS-GR-ZIF-8 (Reproduced with CC BY 4.0[118]. Copyright 2022, MDPI) EESs. ATCl: Acetylthiocholine chloride; AChE: acetylcholinesterase; COF: covalent organic framework; PBS: phosphate buffer solution; DDVP: O,O-dimethyl-O-2,2-dichlorovinylphosphate; GCE: glassy carbon electrode; Tph: 2,5-dihydroxy-1,4-phenyl dicarboxylaldehyde; Dha: 5,10,15,20-tetra(4-aminophenyl)-21H,23H-porphyrin; PDDA: poly (diallyldimethylammonium chloride); OP: organophosphorus pesticide; ZIF-8: zeolitic imidazolate framework-8; GR: graphene; ICP: isocarbophos.

In addition, Yang *et al.*[114] fixed AChE on the surface of PDDA-AuNPs-COFs composites modified GCE by electrostatic interactions between poly (diallyldimethylammonium chloride) (PDDA) and AChE, thereby constructing EESs for the detection of methyl parathion [Figure 5B]. DPV analysis revealed that the inhibition efficiency of the sensors exhibited a good linear relationship with methyl parathion concentration in the range of 1.9-3.8 × 10^4 nM, and the corresponsing LOD was calculated to be 0.23 nM. The recoveries for methyl parathion in tomato and strawberry samples were 95.7%-107.9%. Furthermore, the sensors delivered

outstanding electrochemical detection performance for methyl parathion, including excellent electroactivity, repeatability, stability and selectivity. These superior properties were attributed to the synergistic interaction between the conjugated π-electron macrocycles of porphyrin-based COFs and the conductivity of Au NPs, which facilitated the electron transfer rate of the sensors and thus improved their detection performance.

MOFs-based sensors

The robust binding interaction between Zr^{4+} ion and -P=O/S groups provides Zr-MOFs with high OPs recognition performance, thereby enabling them to serve as the core recognition components in NEESs[87]. More importantly, Zr-MOFs are always used as support materials for immobilizing bioactive enzymes in EESs, duo to their outstanding physicochemical properties such as large specific surface are and good biological compatibility. For this reason, Mahmoudi *et al*.[115] modified GCE with Ce-UiO-66-MWCNTs composites and then immobilized AChE on the surface of the modified electrode to fabricate EESs for paraoxon detection [Figure 5C]. Uder the optimization reaction conditions, DPV results revealed that the suppression rate of the enzymatic sensors displayed a good linear relationship with paraoxon concentration in the LCR of 0.01-150 nM, and the corresponding LOD was calculated to be 0.004 nM. Moreover, electrochemical measurements indicated that the sensors exhibited excellent electrochemical performance, including remarkable stability, selectivity, reproducibility and satisfactory recovery rate in real samples, which was mainly attributed to the polyvalent nature and strong oxophilicity of Ce^{4+}[116]. In addition, MWCNTs facilitated improved electron transfer in the sensor owing to their high electrical conductivity. Meanwhile, UiO-66 contributed to enhanced stability of the sensor due to its high chemical and thermal stability.

Moreover, the Zn^{2+} imidazolate groups possess excellent biological compatibility, making Zn-MOFs suitable supports for the immobilization of biological enzymes[117]. As shown in Figure 5D, Wen *et al*.[118] fabricated EESs by coating AChE-CS-GR-ZIF-8 composites on the surface of GCE using graphene (GR) as the conductive additive and chitosan as the binding agent for isocarbophos detection. Under optimal detection conditions, DPV results revealed that the sensors' peak current decreased with increasing isocarbophos concentration. The LCR was 1.73 - 345.7 nM, and the corresponding LOD was calculated to be 0.62 nM. Additionally, Wu *et al*.[39] constructed EESs by immobilizing AChE-modified amino-functionalized Zn-MOFs on the surface of GCE, with carboxymethyl cellulose applied as a binder for detecting multiple OPs, including glyphosate, fenitrothion, methyl-parathion, trichlorfon, iprobenfos and acephate. Under optimized reaction conditions, electrochemical results demonstrated that the sensors displayed a LCR of 10^{-6}-1 nM for these OPs, with the LOD ranging from 8.75×10^{-5} to 1.24×10^{-4} nM and the LOQ from 4.13×10^{-4} to 1.12×10^{-4} nM, respectively. The sensors were used for the real-time detection of these OPs combined with near-field communication chips. Among these OPs, the sensors presented the best detection performance for glyphosate, which was attributed to the charge redistribution triggered by the specific interaction between amino-functionalized Zn-MOFs and glyphosate[119].

Although POFs possess excellent structural features, including large specific surface area, high porosity and well-defined crystal structures, studies on POFs-based EESs remain fewer than those on POFs-based NEESs. Table 2 systematically summarizes the performance of POFs-based EESs for the detection of OPs. According to Table 2, the enzymatic sensors also exhibit the broad LCR from picomolar to nanomolar level, with the ultralow (LOD) for OPs detection that is significantly lower than that of most NEESs. Similar to NEESs show satisfactory reproducibility and repeatability with an RSD lower than 5%, good anti-interference against common inorganic ions and acids, and acceptable recovery rates in real samples. AchE is the most widely used enzyme for the detection of OPs. However, due to the insufficient thermal stability of its biologically active structure, most enzymatic sensors can only be stored at 4 °C for less than 30 days, with more than 20% loss of initial catalytic activity (i.e., residual activity below 80%). Furthermore, owing to the broad-spectrum

Table 2. The detection performance of EESs for OPs

Sensors	Performance	Ref.
AChE-COF NFs/Homogeneous sensors	LCR for dichlorvos: 10^{-2}-10^{2} ng mL^{-1}; LOD: 1.50 ng·mL^{-1}; Stability (30 days): almost unchanged; Reproducibility (6 electrodes): RSD of 4.2%; Anti-interference capability: ascorbic acid, dopamine, inorganic ions; Recovery rate in real samples: 85.6%-136%	[23]
AChE-COFs-MWCNTs/GCE	LCR for malathion: 1-10^{4} nM; LOD: 0.5 nM; Stability (4 °C): 82.9% of initial activity; Reproducibility (10 electrodes): RSD of 2.19%; Anti-interference capability: inorganic ions; Recovery rate in real samples: 96%-105%	[113]
AChE-PDDA-AuNPs-COFs/GCE	LCR for methyl parathion: 1.9-3.8 × 10^{4} nM; LOD: 0.23 nM; Repeatability (5 times): RSD of 2.4%; Stability (14 days, 4 °C): 92.0% of initial activity; Reproducibility (5 electrodes): RSD of 2.8%; Anti-interference capability: urea, ascorbic acid, glucose, acetamiprid, citric acid, indoxacarb, inorganic ions; Recovery rate in real samples: 95.7%-107.9%	[114]
AChE-COF-3D-KSCs/GCE	LCR for trichlorfon: 0.2-19 ng mL^{-1}; LOD: 0.067 ng mL^{-1}; Stability (30 days, 4 °C): 94% of initial activity; Reproducibility (5 electrodes): RSD of 3.9%; Anti-interference capability: nitrophenol, catechol, hydroquinone, inorganic ions; Recovery rate in real samples: 96.1%-105%	[120]
AChE-Ce-UiO-66-MWCNTs/GCE	LCR for paraoxon: 0.01-150 nM; LOD: 0.004 nM; Repeatability (5 times): RSD of 4.3%; Stability (20 days, 4 °C): 85% of initial activity; Anti-interference capability: glucose, diazinon, carbofuran, carbaryl, 4-nitrophenol, malathion, oxalic acid, citric acid, inorganic ions; Recovery rate in real samples: 95%-102%	[115]
AChE-Zn-MOFs/GCE	LCR for multiple OPs including glyphosate, fenitrothion, trichlorfon, iprobenfos, acephate and methyl-parathion: 10^{-6}-1 nM; LOD: ranging from 8.75 × 10^{-5} to 1.24 × 10^{-4} nM; LOQ: ranging from 4.13 × 10^{-4} to 1.12 × 10^{-4} nM; Anti-interference capability: propoxur, 2,4-d-butyl ester, cypermethrin, ascorbic acid, glucose, uric acid, inorganic ions; Recovery rate in real samples: 87.1%-109.6%	[39]
AChE-CS-GR-ZIF-8/GCE	LCR for isocarbophos: 1.73-345.7 nM; LOD: 0.62 nM; Stability (6 days, 4 °C): 98.09% of initial activity; Reproducibility (5 electrodes: RSD of 5.05%); Anti-interference capability: glucose, urea, inorganic ions; Recovery rate in real samples: 88.1%-122.4%	[116]
AChE-Cys-aAuNR-MOFs/ITO	LCR for chlorpyrifos: 0.03 ng mL^{-1} - 6 ng mL^{-1}; Sensitivity: 2.04 μA ng^{-1} L cm^{-2}; LOD: 0.003 ng mL^{-1}; Stability (15 days): 90.0% of initial activity; Anti-interference capability: diisopropyl fluorophosphate, aflatoxinB1, inorganic ions	[121]

EES: Enzymatic electrochemical sensor; OP: organophosphorus pesticide; AChE: acetylcholinesterase; NF: nanofiber; LCR: linear concentration range; LOD: limit of detection; RSD: relative standard derivations; MWCNT: multi-walled carbon nanotube; GCE: glassy carbon electrode; PDDA: poly (diallyldimethylammonium chloride); NP: nanoparticle; KSC: kenaf stem composite; UiO-66: zirconium 1,4-dicarboxybenzene metal-organic framework; MOF: metal-organic framework; CS: chitosan; GR: graphene; ZIF-8: zeolitic imidazolate framework-8; NR: nanorod; ITO: indium tin oxide.

response of enzymes for OPs, the same enzymatic sensor is often applied for the detection of multiple OPs, including glyphosate, fenitrothion, trichlorfon, iprobenfos, acephate, and methyl parathion, resulting in low selectivity among different OPs. Therefore, to further promote the practical application of EESs, improvements in their storage stability and selectivity toward individual OPs are urgently required.

Other POFs-based electrochemical-related sensors

Besides the construction of mono-signal non-enzymatic/enzymatic electrochemical sensors, POFs as versatile platforms have also been used to fabricate multi-signal electrochemical sensors. These sensors are driven by the combination of electrochemical and other sensing technology, thus realizing the ultrasensitive detection of OPs. For example, based on electrochemical and photothermal technologies, Wen *et al.*[122] prepared dual-modal sensors by modifying GCE with COFs-MB-MnO_2 composites for the complementary detection of chlorpyrifos. The working principle of the sensors is to establish the linear relationship between the concentration of chlorpyrifos and the peak current of MB released from the COFs-MB-MnO_2 composites, as well as the correlation between the concentration of chlorpyrifos and the temperature variation induced by MnO_2-catalyzed oxidation of tetramethylbenzidine, as illustrated in Figure 6A. Combined with electrochemical and photothermal analysis, the dual-modal sensors exhibited high detection performance toward chlorpyrifos. Linear relationships were obtained in the concentration ranges of 0.5-200 ng mL^{-1} for the electrochemical signal and 0-8,000 ng mL^{-1} for the photothermal signal, with the corresponding LODs of 0.0632 and 0.108 ng mL^{-1}, respectively. Additionally, based on the competition

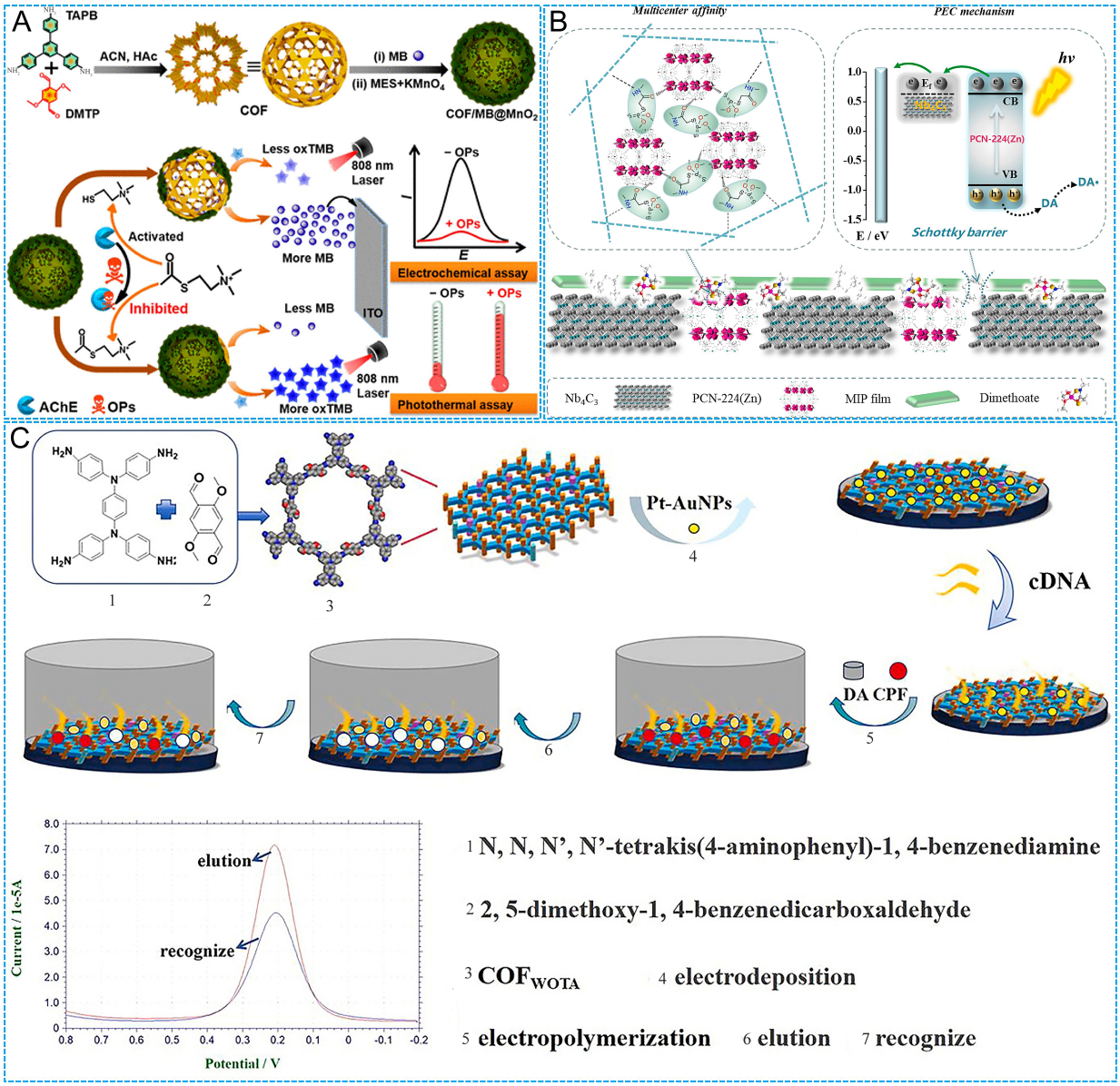

Figure 6. (A) The detection mechanism of dual-modal sensors (Reproduced with permission[122]. Copyright 2023, American Chemical Society); (B) the preparation of PCN-224(Zn) Reproduced with permission[126]. Copyright 2023, Elsevier); (C) PtAu NPs-COFs (Reproduced with permission[127]. Copyright 2025, Elsevier) MIP sensors. TAPB: 1,3,5-tris(4-aminophenyl)benzene; DMTP: 2,5-dimethoxyterephthalic acid; COF: covalent organic framework; MB: methylene blue; MES: 4-morpholineethanesulfonic acid; OP: organophosphorus pesticide; TMB: tetramethylbenzidine; ITO: indium tin oxide; AChE: acetylcholinesterase; PEC: photoelectrochemical; PCN: polycentric; MIP: molecularly imprinted polymer; NP: nanoparticle; DA: dopamine; CPF: chlorpyrifo; PCN-224: porous coordination network-224.

between the formation of Cu-glyphosate complexes and the electrochemical reduction catalytic activity of phenazine-2,3-diyldiamine, Zhao *et al.*[123] coated Cu-Hemin-MOFs-CNTs composites by a one-step electrochemical deposition method on GCE to construct dual-signal electrochemical sensors for glyphosate detection. Electrochemical results revealed that the peak current of the sensors was varied linearly with the glyphosate concentration under optimal detection conditions. For the Cu-glyphosate signal, the LCR was 0.1 - 3.0 × 10^3 nM, with a LOD of 5.17 × 10^{-3} nM. For the phenazine-2,3-diyldiamine signal, the LCR was 0.1-5.0 × 10^4 nM, with a LOD of 6.81 × 10^3 nM. The recoveries for glyphosate in water, soil and tea samples were 98.0%-102.6% for the Cu-glyphosate signal and 97.0%-102.8% for the phenazine-2,3-diyldiamine signal, respectively. The design and assembly of these dual-modal sensors pave the way for the fabrication of novel multi-modal electrochemical sensors and facilitate the real-time detection for OPs in food matrices.

To further expand the application of POFs in the domain of electrochemical sensors, they have been used to prepare other electrochemical-related sensors, such as MIP, APT and ECL sensors. MIP sensors simulate the antigen-antibody interaction to specifically identify target object by using MIP as the recognition element[124]. For instance, Zhong *et al.*[125] assembled Cu-MOFs-Au NPs-rGO-MIP sensors by multistep electrochemical methods, which included the co-electrodeposition of Au NPs and Cu-MOFs, the electroreduction of GO and the electro-polymerization of MIP. Electrochemical results showed that the concentration of phosmet changed linearly with the peak current of the sensors over the LCR of 1.0×10^{-5} - 500 nM, with a LOD of 7.2×10^{-6} nM. Furthermore, by integrating photochemical sensing technology, Ma *et al.*[126] designed and prepared Nb_4C_3 modified PCN-224(Zn)-MOFs-MIP photoelectrochemical sensors for detecting dimethoate, due to the multicenter affinity of photoactive PCN-224(Zn) MOFs for dimethoate [Figure 6B]. The photocurrent of the sensors decreased with increasing dimethoate concentration under optimized operational conditions, presenting a linear relationship in the LCR of 0.1 - 10^3 nM, with a LOD of 2.61×10^4 nM. In addition, Yu *et al.*[127] anchored MIP on the surface of GCE decorated with PtAu NP-COF composites for the detection of chlorpyrifos. To further improve detection performance, APT was integrated into the MIP sensors to construct dual-identification electrochemical sensors [Figure 6C]. Electrochemical analysis showed that the dual-identification sensors displayed high detection performance for chlorpyrifos under optimized detection conditions, with a LCR of 10^{-5} - 1.0 nM, and the calculated LOD was 9.34×10^5 nM. These results demonstrate that MIP sensors have achieved picomolar-level detection of OPs and exhibited great practical application prospect in the field of OPs detection.

Nevertheless, the special binding between target object and APT (such as single-stranded DNA or RNA oligonucleotide) in APT sensors is transformed into electrochemical signal for detecting target object[128]. In virtue of the coupling interaction between the high electronic conductivity of Cu^{2+} and the excellent stability and large surface area of Zr^{4+}, Dong *et al.*[129] fixed thiol-modified APT on GCE (modified by CuZr-MOFs and polyvinyl pyrrolidone stabilized Au NPs) by the strong interaction between Au and S atom for detecting multiple OPs, including phorate, dichlorvos and omethoate [Figure 7A]. Electrochemical analysis indicated that the peak current of the APT sensors was directly proportional to OPs concentration under optimized detection conditions. The calculated LODs were 2.36×10^{-7} nM for phorate, 1.20×10^{-5} nM for omethoate and 4.56×10^{-5} nM for dichlorvos, respectively. Additionally, combined with colorimetric and electrochemical sensing technology, Xu *et al.*[130] developed Fe-MOFs dual-signal APT sensors for malathion detection, as shown in Figure 7B. It was found that the dual-signal sensors displayed ultrahigh sensitivity for detecting malathion under optimal reaction conditions, with a LCR of 10-500 ng mL^{-1}, and the calculated LOD was 4.6 ng mL^{-1} for electrochemical signal and 5.8 ng mL^{-1} for colorimetric signal, respectively. In a word, apt sensors have exhibited ultrahigh sensitivity for OPs detection, but their selectivity still needs to improve for practical application.

ECL is divided into annihilation and co-reactant type[131]. It is well known that the luminous efficiency of co-reactant type ECL is much higher than that of the annihilation type. The luminous process of co-reactant type ECL includes the oxidization/reduction of luminophore on the surface of electrode, the formation of strongly reductive/oxidative free radical by co-reactant, the generation of excited-state species by the reduction/oxidization of oxidative/reductive luminophore, and the release of luminescence when excited-state species return to the ground state[132]. The released luminescence signal is used for detecting food contaminants. Simultaneously, POFs are used as promoters to improve the redox activity of co-reactant, owing to their distinct well-defined porous structure[133]. For instance, by using CdTe quantum dot-decorated Zn-MOFs as luminophores and $K_2S_2O_8$ as co-reactant, Gu *et al.*[134] prepared cathodic electrochemiluminescence sensors for the detection of profenofos, as illustrated in Figure 7C. Under optimal detection conditions, the ECL response intensity was increased linearly with the profenofos concentration, with a LCR of 1.34×10^{-4}-1.34×10^6 nM and a LOD of 4.47×10^{-5} nM. Their high electrochemical

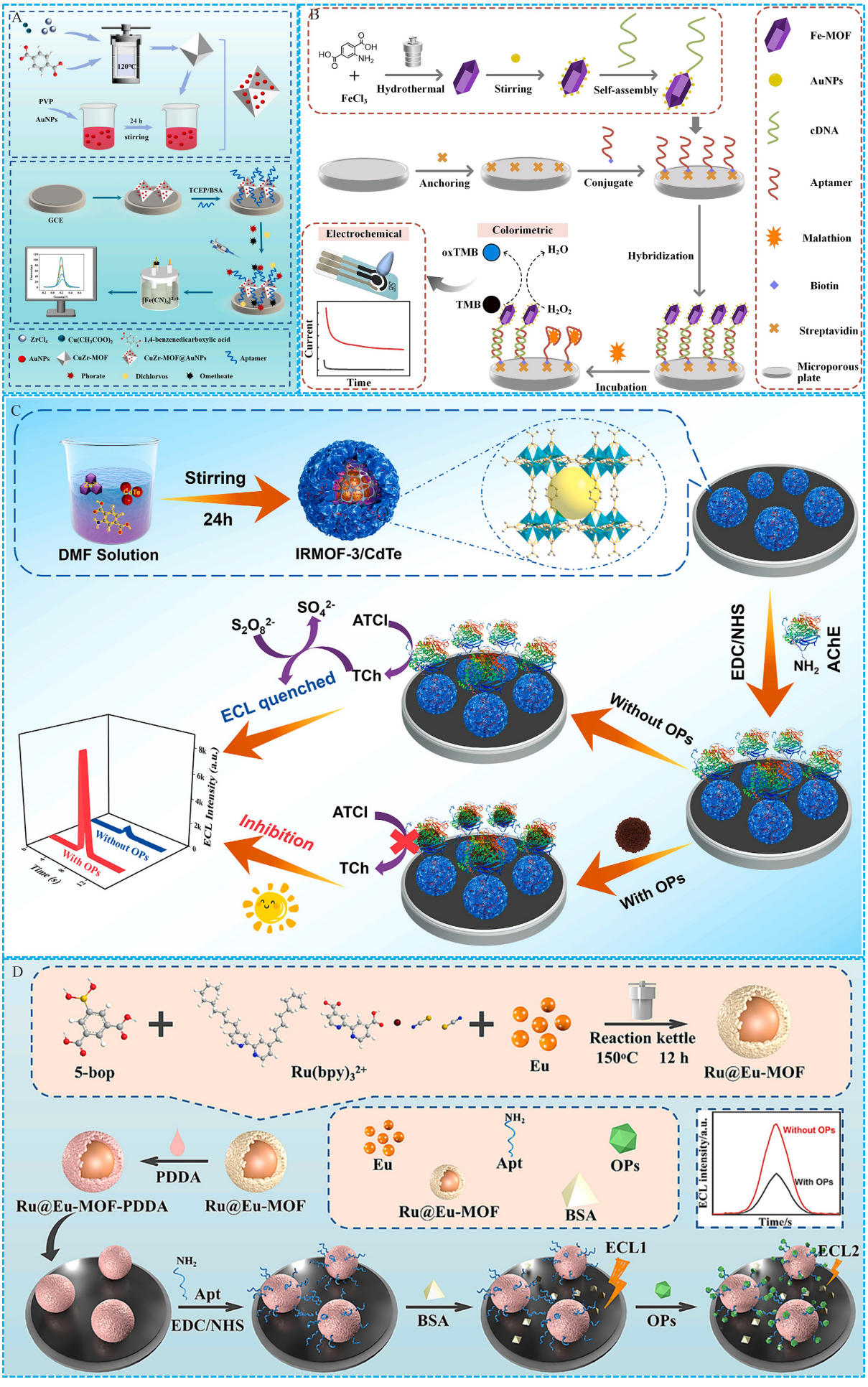
A
120°C
PVP
AuNPs
24 h
stirring
GCE
TCEP/BSA
ZrCl4
Cu(CH3COO)2
1,4-benzenedicarboxylic acid
AuNPs
CuZr-MOF
CuZr-MOF@AuNPs
Aptamer
Phorate
Dichlorvos
Omethoate
B
Hydrothermal
Stirring
Self-assembly
FeCl3
Anchoring
Conjugate
Hybridization
Incubation
Electrochemical
Colorimetric
oxTMB
H2O
TMB
H2O2
Current
Time
Fe-MOF
AuNPs
cDNA
Aptamer
Malathion
Biotin
Streptavidin
Microporous plate
C
Stirring
24h
DMF Solution
IRMOF-3/CdTe
S2O8 2-
SO4 2-
ATCl
TCh
ECL quenched
Without OPs
EDC/NHS
NH2
AChE
ECL Intensity (a.u.)
Time (s)
With OPs
Inhibition
D
5-bop
Ru(bpy)3 2+
Eu
Reaction kettle
150°C 12 h
Ru@Eu-MOF
PDDA
Ru@Eu-MOF-PDDA
Apt
OPs
BSA
ECL intensity/a.u.
Time/s
ECL1
ECL2

Figure 7. (A) The preparation of CuZr-MOFs (Reproduced with permission [129]. Copyright 2025, Academic Press); (B) Fe-MOFs (Reproduced with permission[130]. Copyright 2024, Elsevier) APT sensors; (C) The preparation of Zn-MOFs (Reproduced with permission[134]. Copyright 2025, Elsevier), Ru-Eu-MOFs (D) Reproduced with permission[135]. Copyright 2025, Elsevier) ECL sensors. MOF: metal organic framework; NP: nanoparticle; PVP: polyvinyl pyrrolidone; TCEP: tis(2-chloroethyl) phosphate; BSA: bovine serum albumin; TMB: 3,3',5,5'-tetramethyl benzidine; DMF: N, N-dimethylformamide; OP: organophosphorus pesticide; AchE: acetylcholinesterase; ARCI: acetylcholinesterase; EDC: 1-Ethyl-(3-dimethylaminopropyl) carbodiimide; ECL: electrochemiluminescence; NHS: N-hydroxy succinimide; PDDA: poly (diallyldimethylammonium chloride); APT: aptamer based.

performance might be attributed to the high capture and catalytic ability of CdTe quantum dot-decorated Zn-MOFs. In addition, Shen *et al.*[135] immobilized tris (2, 2' -bipyridyl) ruthenium (II) on the surface of PDDA-modified dual-ligand Eu-MOFs to prepare luminescent materials, and thus constructed ECL sensors by multiple-step assemble methods involving the immobilization of amino-decorated APT and the inhibition of bovine serum albumin, as shown in Figure 7D. Using TPrA as co-reactant, the ECL sensors exhibited high detection performance for four OPs under optimal reaction conditions. The calculated LODs were 0.0482 ng mL^{-1} for phorate, 0.0093 ng mL^{-1} for profenofos, 0.0085 ng mL^{-1} for isocarbophos and 0.0893 ng mL^{-1} for omethoate, respectively. These findings indicate that ECL sensing is an effective strategy for the detection of OPs, but the preparation process of ECL sensors need to be further simplified to promote their practical application in real-time OPs detection.

SUMMARY AND OUTLOOK

The dimensional classifications and preparation technologies of POFs, as well as their advancements in electrochemical sensing for OPs, were systematically summarized in this review. Numerous POFs-based electrochemical sensors have been developed for detection OPs. Their LCR ranged from picomolar to micromolar, and their LOD was as low as picomolar. The RSD values of both repeatability and reproducibility were below 5%, and the recovery rate in real samples ranged from 90% to 120%. The as-fabricated sensors exhibited excellent electrochemical detection performance for OPs, but their storage stability still requires further improvement, with the sensors retaining roughly 80%-95% of their initial activity after storage at 4 °C for one to four weeks. Although significant breakthroughs have been achieved in the construction of POFs-based electrochemical sensors, this field remains in its infancy, and numerous challenges must be addressed prior to their large-scale application. Therefore, prospective research directions are proposed toward the development of POFs-based electrochemical sensors with outstanding detection performance, including excellent selectivity, stability, sensitivity and satisfactory reproducibility, as detailed in the following aspects.

(1) As is well known, POFs represent one of the most critical components in electrochemical sensors. Their intrinsic structural and compositional stability is closely correlated with both the stable electrochemical response of sensors under operating conditions and their storage stability. Therefore, it is highly significant to elucidate the stability mechanism of POFs under these conditions and establish the relationship between their structural/compositional stability and various synthetic parameters, thereby developing green, rapid and cost-effective preparation technologies for the large-scale production of highly stable POFs with controllable composition and structure.

(2) The combination of theoretical methods (including first-principles calculations and molecular dynamics simulations) and high-resolution characterization techniques (such as in-situ infrared/Raman spectroscopy, X-ray absorption spectroscopy, and spherical aberration-corrected electron microscopy) can be employed to deeply analyze the electrochemical mechanism of POFs in NEESs for target OPs detection, and to reveal the correlation between sensor detection performance and the characteristic structural and compositional parameters of POFs. Based on the mechanistic analysis and identification of the key parameters governing the detection performance, machine learning can be utilized to rationally design high-performance POFs for target OPs, thereby fabricating high-performance NEESs for the specific detection of target OPs.

(3) Bioactive enzymes serve as core components of EESs. Investigating the interaction mechanism between POFs and bioactive enzymes is critical for enhancing the immobilization stability of bioactive enzymes, thereby enabling the construction of high-performance EESs for the detection of OPs detection. In addition, through in-depth exploration of the active structures of bioactive enzymes toward OPs, the design and preparation of biomimetic enzymes via biomimetic methods may be another promising route to develop high-stability electrochemical sensors for OP detection.

(4) To further improve their detection performance for OPs, numerous novel integration strategies need to be developed to construct advanced electrochemical-related sensors. Investigating the integration mechanism between electrochemistry and other detection techniques is critical for fabricating multimodal electrochemical-related sensors for the ultrasensitive detection of OPs.

In summary, through continuous efforts, high-performance POF-based electrochemical sensors will be developed to realize rapid, efficient, and low-cost real-time detection of OPs. In addition, as one of the most promising emerging materials, POFs will attract increasing attention in various application fields.

DECLARATIONS

Authors' contributions

Writing-original draft, writing-review & editing: Chen, Z.; Ma, S.
Writing-review & editing: He, H.
Collecting the literature, Data curation: Yao, T.; Yu, Y.; Xiong, L.
Data curation: Wang, S.; Fan, T.
Conceptualization, Supervision, Writing-review & editing, Funding acquisition: Hong, X.; Wang, G.

Availability of data and materials

Not applicable.

AI and AI-assisted tools statement

During the revision of this manuscript, the Bean Bun AI (ByteDance, released 2025-12-01) and Tianxi Personal Super Intelligent Agent (Lenovo, released 2025-05-07) were used solely for language editing. These tools did not influence the scientific content of the work. All authors take full responsibility for the accuracy, integrity, and final content of the manuscript.

Financial support and sponsorship

This work was supported by the National Natural Science Foundation of China [grant number 32072304], Guangdong Basic and Applied Basic Research Foundation (grant numbers 2023A1515140180, 2022A1515140159, 2024A1515012826), Key Project in the Field of Biomedicine and Health (Food) by Department of Education of Guangdong Province (grant number 2025ZDZX2067), Innovation team project of general colleges in Guangdong Province (grant number 2024KCXTD044), Guangdong Province Key Construction Discipline Research Ability Improvement Project (grant number 2024ZDJS027).

Conflicts of interest

All authors declared that there are no conflicts of interest.

Ethical approval and consent to participate

Not applicable.

Consent for publication

Not applicable.

REFERENCES

1. Castelvecchi, D.; Naddaf, M. Chemistry Nobel for scientists who developed massively porous 'super sponge' materials. *Nature* **2025**, *646*, 522-3. DOI
2. Hoskins, B. F.; Robson, R. Infinite polymeric frameworks consisting of three dimensionally linked rod-like segments. *J. Am. Chem. Soc.* **2002**, *111*, 5962-4. DOI
3. Yaghi, O. M.; Li, G.; Li, H. Selective binding and removal of guests in a microporous metal-organic framework. *Nature* **1995**, *378*, 703-6. DOI
4. Côté, A. P.; Benin, A. I.; Ockwig, N. W.; O'Keeffe, M.; Matzger, A. J.; Yaghi, O. M. Porous, crystalline, covalent organic frameworks. *Science* **2005**, *310*, 1166-70. DOI
5. Singh, A.; K K, S.; Bhatnagar, A.; Gupta, A. K. Crystalline porous frameworks: advances in synthesis, mechanisms, modifications, and remediation of organic pollutants. *Sep. Purif. Technol.* **2025**, *353*, 128588. DOI
6. Jiao, L.; Seow, J. Y. R.; Skinner, W. S.; Wang, Z. U.; Jiang, H. Metal-organic frameworks: Structures and functional applications. *Materials. Today.* **2019**, *27*, 43-68. DOI
7. Abuzeid, H. R.; El-mahdy, A. F.; Kuo, S. Covalent organic frameworks: design principles, synthetic strategies, and diverse applications. *Giant* **2021**, *6*, 100054. DOI
8. Larsen, A. E.; Noack, F.; Powers, L. C. Spillover effects of organic agriculture on pesticide use on nearby fields. *Science* **2024**, *383*, eadf2572. DOI
9. Abubakar, Y., Tijjani, H., Egbuna, C., et al. Pesticides, history, and classification. In *Natural Remedies for Pest, Disease and Weed Control*; Elsevier, 2020; pp 29-42. DOI
10. Zhang, Z.; Zhang, Y.; Jayan, H.; et al. Recent and emerging trends of metal-organic frameworks (MOFs)-based sensors for detecting food contaminants: a critical and comprehensive review. *Food. Chem.* **2024**, *448*, 139051. DOI
11. Ganie, S. Y.; Javaid, D.; Hajam, Y. A.; Reshi, M. S. Mechanisms and treatment strategies of organophosphate pesticide induced neurotoxicity in humans: a critical appraisal. *Toxicology* **2022**, *472*, 153181. DOI
12. Musa Jaber Al-Maliki, A.; Masrournia, M.; Sanavi Khoshnood, R.; Beyramabadi, A. Dispersive micro solid-phase extraction with bimetallic Ni, Zn-MOF sorbent and gas chromatography method for organophosphorus pesticide determination in environmental water samples. *Microchem. J.* **2024**, *205*, 111259. DOI
13. Jafari, M.; Gholami, A.; Akhgari, M. A novel method for the determination of organophosphorus pesticides in urine samples using a combined gas diffusion microextraction (GDME) and gas chromatography-mass spectrometry (GC-MS) technique. *MethodsX* **2025**, *14*, 103212. DOI
14. Zhang, S.; You, Q.; Zhuo, X.; et al. Rapid and simple determination of organophosphorus pesticides in urine using polydopamine-modified monolithic spin column extraction combined with liquid chromatography-mass spectrometry. *J. Chromatogr. A.* **2023**, *1696*, 463959. DOI
15. Shi, R.; Li, J.; Yu, W.; et al. Biotinylated fusion protein-streptavidin-peroxidase complex based non-competitive magnetic immunoassay for rapid detection of organophosphorus pesticides. *Talanta. Open.* **2025**, *12*, 100483. DOI
16. Wang, J.; Zeng, Q.; Cao, K.; Cui, Y.; Xiao, H.; Wang, L. Green synthesis of hawthorn polysaccharide-stabilized Pd@Ru nanozymes for sensitive colorimetric detection of organophosphorus pesticides. *Int. J. Biol. Macromol.* **2025**, *329*, 147780. DOI
17. Zhou, C.; Feng, J.; Tian, Y.; et al. Non-enzymatic electrochemical sensors based on nanomaterials for detection of organophosphorus pesticide residues. *Environ. Sci.:. Adv.* **2023**, *2*, 933-56. DOI
18. Kumaravel, A.; Chandrasekaran, M. Electrochemical determination of chlorpyrifos on a nano-TiO_2/cellulose acetate composite modified glassy carbon electrode. *J. Agric. Food. Chem.* **2015**, *63*, 6150-6. DOI
19. Zhang, Y.; Wang, X.; Wang, Y.; Xu, N.; Wang, X. Anderson-type polyoxometalate-based sandwich complexes bearing a new "V"-like bis-imidazole-bis-amide ligand as electrochemical sensors and catalysts for sulfide oxidation. *Polyoxometalates* **2022**, *1*, 9140004. DOI
20. Liu, X. L.; Guo, J. W.; Wang, Y. W.; Wang, A. Z.; Yu, X.; Ding, L. H. A flexible electrochemical sensor for paracetamol based on porous honeycomb-like NiCo-MOF nanosheets. *Rare. Metals.* **2023**, *42*, 3311-7. DOI
21. Sumithra, B.; Saravanan, V.; Ramalingan, C.; Sivaganesh, D.; Lakshmanan, P.; Geetha, D. Harnessing sunlight: unlocking superior photocatalytic activity of g-C_3N_4/$MnWO_4$ heterojunction photocatalysts for degradation of hazardous compounds. *Tungsten* **2024**, *7*, 255-67. DOI
22. Duan, S.; Wu, X.; Shu, Z.; et al. Curcumin-enhanced MOF electrochemical sensor for sensitive detection of methyl parathion in vegetables and fruits. *Microchem. J.* **2023**, *184*, 108182. DOI
23. Wang, L.; Wu, N.; Wang, L.; Song, Y.; Ma, G. Accurate detection of organophosphorus pesticides based on covalent organic framework nanofiber with a turn-on strategy. *Sensor. Actuat. B-Chem.* **2022**, *372*, 132608. DOI

24. Nangare, S. N.; Patil, S. R.; Patil, A. G.; et al. Structural design of nanosize-metal-organic framework-based sensors for detection of organophosphorus pesticides in food and water samples: current challenges and future prospects. *J. Nanostruct. Chem.* **2021**, *12*, 729-64. DOI
25. Lu, Z.; Wang, Y.; Li, G. Covalent organic frameworks-based electrochemical sensors for food safety analysis. *Biosensors* **2023**, *13*, 291. DOI PubMed PMC
26. Zheng, H.; Yan, W.; Zhang, J. Porous organic framework-based materials (MOFs, COFs and HOFs) for lithium-/sodium-/potassium-/zinc-/aluminum-/calcium-ion batteries: a review. *Electrochem. Energy. Rev.* **2025**, *8*, 3. DOI
27. Huang, P.; Hou, L. H.; Yang, M. Y.; et al. One-dimensional covalent organic frameworks: from design, synthesis to applications. *Angew. Chem. Int. Ed.* **2025**, *64*, e202507002. DOI
28. Dai, Y.; Zhang, G.; Peng, Y.; Li, Y.; Chi, H.; Pang, H. Recent progress in 1D MOFs and their applications in energy and environmental fields. *Adv. Colloid. Interface. Sci.* **2023**, *321*, 103022. DOI
29. Pan, X.; Zhu, Q.; Yu, K.; et al. One-dimensional metal-organic frameworks: synthesis, structure and application in electrocatalysis. *Next. Mater.* **2023**, *1*, 100010. DOI
30. Pezhhanfar, S.; Farajzadeh, M. A.; Hosseini-Yazdi, S. A.; Mogaddam, M. R. A. An all-embracing analytical method comprising modified QuEChERS-dispersive micro-solid-phase extraction-dispersive liquid-liquid microextraction using FeGA MOF for the extraction and preconcentration of pesticides simultaneously from juice and flesh of watermelon. *Anal. Sci.* **2023**, *39*, 1201-14. DOI
31. Jia, T.; Zheng, Z.; Hou, L.; et al. Rational design and synergistic optimization of 2D COF nanofiltration membranes: A review. *J. Environ. Chem. Eng.* **2025**, *13*, 120507. DOI
32. Patil, P. D.; Gargate, N.; Tiwari, M. S.; Nadar, S. S. Two-dimensional metal-organic frameworks (2D-MOFs) as a carrier for enzyme immobilization: A review on design and bio-applications. *Int. J. Biol. Macromol.* **2025**, *291*, 138984. DOI
33. Abdelnasser, E.; Ramadan, A. E. M.; Ifthikar, J.; et al. Opportunities of covalent organic frameworks (COFs) as a promising antibacterial agent. *J. Mol. Struct.* **2026**, *1353*, 144777. DOI
34. Li, R.; Sun, F.; Liu, Z.; Shi, Y.; He, S.; Chen, J. Research progress and prospect of covalent organic frameworks (COFs) and composites: From synthesis to application in water contaminants. *J. Environ. Chem. Eng.* **2024**, *12*, 113944. DOI
35. Dong, X.; Fan, M.; Zhao, L.; Wang, K.; Hu, Z.; Liu, X. Recent advances in MOFs based hydrogels: From interactions, synthesis, and functionalization to food applications. *Trends. Food. Sci. Technol.* **2025**, *166*, 105415. DOI
36. Li, H.; Eddaoudi, M.; O'keeffe, M.; Yaghi, O. M. Design and synthesis of an exceptionally stable and highly porous metal-organic framework. *Nature* **1999**, *402*, 276-9. DOI
37. Xiong, S.; Cui, X.; Guo, J.; et al. Triphenylamine-based covalent organic framework nanospheres: Solvothermal synthesis and electrochromic properties. *J. Electroanal. Chem.* **2023**, *942*, 117563. DOI
38. Wang, X.; Ma, Y.; Ru, J.; et al. One-step solvent thermal synthesis of 3D networked MOF composites for preparation of an ultrasensitive chemosensor for hydroquinone and catechol. *Microchim. Acta.* **2024**, *191*, 274. DOI
39. Wu, Q.; Wang, Y.; Wang, L.; et al. A portable electrochemical biosensor based on an amino-modified ionic metal-organic framework for the one-site detection of multiple organophosphorus pesticides. *ACS. Appl. Mater. Interfaces.* **2024**, acsami.4c13087. DOI
40. Li, W.; Zhang, X.; Zhang, C.; et al. Exploring the corrosion resistance of epoxy coated steel by integrating mechanochemical synthesized 2D covalent organic framework. *Prog. Org. Coat.* **2021**, *157*, 106299. DOI
41. Wang, Z.; Xie, S.; Zhang, W.; et al. Mechanochemical synthesis ionic covalent organic frameworks/cotton composites for pipette tip solid-phase extraction of domoic acid in seafood. *Talanta* **2024**, *269*, 125485. DOI
42. Zhu, Z.; Zheng, Q. Investigation of cryo-adsorption hydrogen storage capacity of rapidly synthesized MOF-5 by mechanochemical method. *Int. J. Hydrogen. Energy.* **2023**, *48*, 5166-74. DOI
43. Ji, W.; Guo, Y.; Xie, H.; Wang, X.; Jiang, X.; Guo, D. Rapid microwave synthesis of dioxin-linked covalent organic framework for efficient micro-extraction of perfluorinated alkyl substances from water. *J. Hazard. Mater.* **2020**, *397*, 122793. DOI
44. Mahmoud, M. M. Microwave-assisted fast synthesis of MOF-801. *Next. Mater.* **2025**, *6*, 100316. DOI
45. Liu, H.; Zhao, Y.; Zhou, C.; Mu, B.; Chen, L. Microwave-assisted synthesis of Zr-based metal-organic framework (Zr-fum-fcu-MOF) for gas adsorption separation. *Chem. Phys. Lett.* **2021**, *780*, 138906. DOI
46. Li, W.; Wu, C.; Zhang, Y.; Guo, H.; Zhao, Z.; Chen, M. Microwave-assisted solvothermal synthesis of cube-shaped MOF-COF composites for copper detection and capture. *Microchem. J.* **2023**, *191*, 108925. DOI
47. Maschita, J.; Banerjee, T.; Savasci, G.; Haase, F.; Ochsenfeld, C.; Lotsch, B. V. Ionothermal synthesis of imide-linked covalent organic frameworks. *Angew. Chem. Int. Ed.* **2020**, *59*, 15750-8. DOI
48. Huang, Z.; Zhang, L.; Cao, P.; Wang, N.; Lin, M. Electrochemical sensing of dopamine using a Ni-based metal-organic framework modified electrode. *Ionics* **2021**, *27*, 1339-45. DOI
49. Kuchekar, S.; Gaikwad, S.; Han, S. Novel ionothermal synthesis of PZ-MIL-101 (Cr) at low temperature for CO_2 and VOCs adsorption. *J. Environ. Chem. Eng.* **2025**, *13*, 116884. DOI

50. Liu, Y.; Zhang, Y.; Zhu, X.; Luan, J.; Lan, Y.; Li, W. Fabrication of a novel 3D cadmium-organic framework doped with europium as multifunctional fluorescence probes for enhancing detectability. *J. Solid. State. Chem.* **2024**, *337*, 124814. DOI
51. Wei, X.; Bi, M.; Lou, Q.; Di, D.; Liu, B.; Pei, D. Fast and facile sonochemical fabrication of covalent organic frameworks in water for the adsorption of flavonoids: adsorption behaviors and mechanisms. *Colloid. Surface. A.* **2024**, *702*, 134731. DOI
52. Vaitsis, C.; Kanellou, E.; Pandis, P. K.; et al. Sonochemical synthesis of zinc adipate metal-organic framework (MOF) for the electrochemical reduction of CO_2: MOF and circular economy potential. *Sustainable. Chem. Pharm.* **2022**, *29*, 100786. DOI
53. Yu, K.; Lee, Y.; Seo, J. Y.; Baek, K.; Chung, Y.; Ahn, W. Sonochemical synthesis of Zr-based porphyrinic MOF-525 and MOF-545: Enhancement in catalytic and adsorption properties. *Microporous. Mesoporous. Mater.* **2021**, *316*, 110985. DOI
54. Xie, C.; Li, H.; Niu, B.; Guo, H.; Lin, X. Comparison of ultrasonic vs mechanochemistry methods for fabrication of mixed-ligand Zn-based MOFs for electrochemical determination of luteolin. *J. Alloys. Compd.* **2024**, *989*, 174363. DOI
55. Qing, Q.; Luo, J.; Liu, S.; et al. General synthesis of covalent organic frameworks under ambient condition within minutes via microplasma electrochemistry approach. *Nat. Commun.* **2025**, *16*, 2571. DOI PubMed PMC
56. Asghar, A.; Iqbal, N.; Noor, T.; Kariuki, B. M.; Kidwell, L.; Easun, T. L. Efficient electrochemical synthesis of a manganese-based metal-organic framework for H_2 and CO_2 uptake. *Green. Chem.* **2021**, *23*, 1220-7. DOI
57. Zhang, Y.; Li, N.; Xu, Y.; et al. An ultra-sensitive electrochemical aptasensor based on Co-MOF/ZIF-8 nano-thin-film by the *in-situ* electrochemical synthesis for simultaneous detection of multiple biomarkers of breast cancer. *Microchem. J.* **2023**, *187*, 108316. DOI
58. Vehrenberg, J.; Vepsäläinen, M.; Macedo, D. S.; Rubio-Martinez, M.; Webster, N. A.; Wessling, M. Steady-state electrochemical synthesis of HKUST-1 with polarity reversal. *Microporous. Mesoporous. Mater.* **2020**, *303*, 110218. DOI
59. Ben, H.; Du, W.; Zhao, J.; et al. Ionic covalent organic frameworks: From synthetic strategies to advanced electro-, photo-, and thermo-energy functionalities. *Coord. Chem. Rev.* **2024**, *517*, 216003. DOI
60. Lalchawimawia, B.; Sil, A.; Banerjee, T.; et al. Metal-organic framework-pesticide interactions in water: Present and future perspectives on monitoring, remediation and molecular simulation. *Coord. Chem. Rev.* **2023**, *490*, 215214. DOI
61. Akmal, M.; Iqbal, M. A.; Mawat, T. H.; et al. Synthesis of metal organic frameworks (MOFs) mechanochemically. *Inorg. Chem. Commun.* **2025**, *175*, 114105. DOI
62. Sud, D.; Kaur, G. A comprehensive review on synthetic approaches for metal-organic frameworks: From traditional solvothermal to greener protocols. *Polyhedron* **2021**, *193*, 114897. DOI
63. Gedye, R.; Smith, F.; Westaway, K.; et al. The use of microwave ovens for rapid organic synthesis. *Tetrahedron. Lett.* **1986**, *27*, 279-82. DOI
64. Gaber, A.; Bilge, S.; Donar, Y. O.; Özoylumlu, B.; Kara, Z.; Sınağ, A. A first comprehensive review of ionothermal carbon-based supercapacitors. *J. Power. Sources.* **2025**, *653*, 237760. DOI
65. Wang, L.; Du, H.; Wang, X.; et al. A critical review of COFs-based photocatalysis for environmental remediation. *Environ. Res.* **2025**, *272*, 121166. DOI
66. Tiong, T.; Chu, J. K.; Tan, K. W. Advancements in acoustic cavitation modelling: progress, challenges, and future directions in sonochemical reactor design. *Ultrason. Sonochem.* **2025**, *112*, 107163. DOI PubMed PMC
67. Jajko-Liberka, G.; Anagha, M.; Chytrosz-Wróbel, P.; et al. Sonochemical synthesis of nanoparticles from bioactive compounds: advances, challenges, and future perspectives. *Ultrason. Sonochem.* **2025**, *121*, 107559. DOI PubMed PMC
68. Guniyangodage Dona, R. L.; Rathuwadu, N. P.; Koswattage, K. R. Electrochemical synthesis methods for polyaniline nanocomposites: Review. *Eur. Polym. J.* **2025**, *241*, 114374. DOI
69. Fenniche, F.; Khane, Y.; Henni, A.; Aouf, D.; Elhak Djafri, D. Synthesis and characterization of PANI nanofibers high-performance thin films via electrochemical methods. *Results. Chem.* **2022**, *4*, 100596. DOI
70. Khaleque, M. A.; Aly Saad Aly, M.; Khan, M. Z. H. Chemical and electrochemical synthesis of doped conducting polymers and their application in supercapacitors: An overview. *Chem. Eng. J.* **2025**, *507*, 160444. DOI
71. Jia, M.; Zhang, W.; Cai, X.; et al. Re-understanding the galvanostatic intermittent titration technique: pitfalls in evaluation of diffusion coefficients and rational suggestions. *J. Power. Sources.* **2022**, *543*, 231843. DOI
72. Wang, X.; Jiang, M.; Yang, P.; et al. Recent advances in pulsed electrochemical techniques: synthesis of electrode materials and electrocatalytic reactions. *Surf. Interf.* **2024**, *50*, 104519. DOI
73. Turan, R.; Bilgen, E.; Koca, A. Electrode modifications with electrophoretic deposition methods for water electrolyzers. *Int. J. Hydrogen. Energy.* **2024**, *81*, 675-706. DOI
74. Fan, T.; Yan, Z.; Huang, W.; et al. A comprehensive review of contents, toxic effects, metabolisms, and environmental behaviors of brominated and organophosphorus flame retardants. *J. Hazard. Mater.* **2025**, *496*, 139428. DOI
75. Sagar, V.; Kukkar, D. Facile adsorption of organophosphate pesticides over HKUST-1 MOFs. *Environ. Monit. Assess.* **2023**, *195*, 1056. DOI

76. Yang, C.; Wang, J.; Yan, W.; Xia, Y. Facile synthesis disposable MOF membrane filter: Growth of NH2-MIL-125 (Ti) on filter paper for fast removal of organophosphorus pesticides in aqueous solution and vegetables. *Food. Chem.* **2022**, *389*, 133056. DOI
77. Yang, Q.; Wang, J.; Zhang, W.; et al. Interface engineering of metal organic framework on graphene oxide with enhanced adsorption capacity for organophosphorus pesticide. *Chem. Eng. J.* **2017**, *313*, 19-26. DOI
78. Zhao, Y.; Qin, K.; Zhou, Y.; Liu, W.; Gao, Z.; Peng, Y. Hierarchically porous Cu-MOF fiber membrane enables instantaneous and continuous removal of organophosphorus pesticides in water. *J. Environ. Chem. Eng.* **2025**, *13*, 115877. DOI
79. Rasheed, T.; Anwar, M. T.; Ahmad, R.; et al. Tailored covalent organic framework-based heterostructures for integrated electrochemical water splitting and reduction reactions: Interfacial design and charge transfer optimization. *J. Alloys. Compd.* **2025**, *1041*, 183889. DOI
80. Rahsepar, F. R.; Farajzadeh, M.; Ansari, F.; Shabani, A. A comprehensive review of engineering g-C_3N_4-based hybrid electrocatalysts via integration of carbon materials and MOF-derived nanostructures for OER, HER, and ORR applications. *Fuel* **2026**, *406*, 137180. DOI
81. Li, F.; Liu, R.; Dubovyk, V.; Ran, Q.; Zhao, H.; Komarneni, S. Rapid determination of methyl parathion in vegetables using electrochemical sensor fabricated from biomass-derived and β-cyclodextrin functionalized porous carbon spheres. *Food. Chem.* **2022**, *384*, 132643. DOI
82. Huang, P.; Wu, W.; Li, M.; et al. Metal-organic framework-based nanoarchitectonics: a promising material platform for electrochemical detection of organophosphorus pesticides. *Coord. Chem. Rev.* **2024**, *501*, 215534. DOI
83. Qi, P.; Wang, J.; Li, H.; et al. Fluffy ball-like magnetic covalent organic frameworks for adsorption and removal of organothiophosphate pesticides. *Sci. Total. Environ.* **2022**, *840*, 156529. DOI
84. Zhang, X.; Hao, N.; Liu, S.; et al. Construction of phosphatase-like COF-OMe@Valine-CeO_2 nanozymes for ultrasensitive electrochemical detection of organophosphorus pesticides. *Sensor. Actuat. B-Chem.* **2024**, *417*, 136068. DOI
85. Gao, N.; Tan, R.; Cai, Z.; Zhao, H.; Chang, G.; He, Y. A novel electrochemical sensor via Zr-based metal organic framework-graphene for pesticide detection. *J. Mater. Sci.* **2021**, *56*, 19060-74. DOI
86. Cao, Y.; Wang, L.; Shen, C.; Wang, C.; Hu, X.; Wang, G. An electrochemical sensor on the hierarchically porous Cu-BTC MOF platform for glyphosate determination. *Sensor. Actuat. B-Chem.* **2019**, *283*, 487-94. DOI
87. Patel, R.; Gupta, R.; Kushwaha, H. S. Non-enzymatic electrochemical sensing of glyphosate pesticide using nickel-based metal-organic framework. *Electrocatalysis* **2025**, *16*, 404-13. DOI
88. Dey, B.; Ahmad, M. W.; Syed, A.; Bahkali, A. H.; Verma, M.; Choudhury, A. Iron metal organic framework decorated carbon nanofiber-based electrode for electrochemical sensing platform of chlorpyrifos in fruits and vegetables. *Mater. Sci. Semicond. Process.* **2024**, *181*, 108669. DOI
89. Yassin, J. M.; Taddesse, A. M.; Tsegaye, A. A.; Sánchez-Sánchez, M. CdS/g-C_3N_4/Sm-BDC MOF nanocomposite modified glassy carbon electrodes as a highly sensitive electrochemical sensor for malathion. *Appl. Surf. Sci.* **2024**, *648*, 158973. DOI
90. Janjani, P.; Bhardwaj, U.; Gupta, R.; Singh Kushwaha, H. Bimetallic Mn/Fe MOF modified screen-printed electrodes for non-enzymatic electrochemical sensing of organophosphate. *Anal. Chim. Acta.* **2022**, *1202*, 339676. DOI
91. Abedeen, M. Z.; Laddha, H.; Sharma, M.; Gupta, R.; Kushwaha, H. S. Non-enzyme picomolar sensing of acephate by modified glassy carbon electrode using bimetallic Zn-Cu metal-organic framework. *J. Electroanal. Chem.* **2023**, *948*, 117810. DOI
92. Sankhla, L.; Abedeen, M. Z.; Gupta, R.; Kushwaha, H. S. Screen-printed bimetallic cobalt-manganese metal-organic framework electrodes for electrochemical detection of dichlorvos. *J. Electrochem. Soc.* **2024**, *171*, 066505. DOI
93. Zhu, X.; Li, B.; Yang, J.; et al. Effective adsorption and enhanced removal of organophosphorus pesticides from aqueous solution by Zr-based MOFs of UiO-67. *ACS. Appl. Mater. Interfaces.* **2014**, *7*, 223-31. DOI
94. Gokila, N.; Haldorai, Y.; Saravanan, P.; Rajendra Kumar, R. T. Non-enzymatic electrochemical impedance sensor for selective detection of electro-inactive organophosphate pesticides using Zr-MOF/ZrO_2/MWCNT ternary composite. *Environ. Res.* **2024**, *251*, 118648. DOI
95. Han, J.; Li, F.; Zhao, M.; et al. Ultrasensitive electrochemical sensing platform based on Zr-based MOF embellished single-wall carbon nanotube networks for trace analysis of methyl parathion. *Microchem. J.* **2024**, *200*, 110323. DOI
96. Guo, M.; Li, F.; Ran, Q.; et al. Facile fabrication of Zr-based metal-organic framework/Ketjen black-carbon nanotubes composite sensor for highly sensitive detection of methyl parathion. *Microchem. J.* **2023**, *190*, 108709. DOI
97. Khoshsafar, H.; Karimian, N.; Nguyen, T. A.; et al. Enzymeless voltammetric sensor for simultaneous determination of parathion and paraoxon based on Nd-based metal-organic framework. *Chemosphere* **2022**, *292*, 133440. DOI
98. Sheals, J.; Persson, P.; Hedman, B. IR and EXAFS Spectroscopic studies of glyphosate protonation and copper(II) complexes of glyphosate in aqueous solution. *Inorg. Chem.* **2001**, *40*, 4302-9. DOI
99. Zhang, C.; Han, M.; Yu, L.; Qu, L.; Li, Z. Fabrication an electrochemical sensor based on composite of Cu-TCPP nanosheets and PSS functionalized graphene for simultaneous and sensitive determination of dihydroxybenzene isomers. *J. Electroanal. Chem.* **2021**, *890*, 115232. DOI

100. Jiang, R.; Pang, Y.; Yang, Q.; Wan, C.; Shen, X. Copper porphyrin metal-organic framework modified carbon paper for electrochemical sensing of glyphosate. *Sensor. Actuat. B-Chem.* **2022**, *358*, 131492. DOI
101. Dey, B.; Ahmad, M. W.; Kim, B. H.; et al. Manganese cobalt-MOF@carbon nanofiber-based non-enzymatic histamine sensor for the determination of food freshness. *Anal. Bioanal. Chem.* **2023**, *415*, 3487-501. DOI
102. Dey, B.; Kushwaha, K. S.; Choudhury, A.; et al. Novel non-enzymatic electrochemical sensing platform based on copper metal organic frameworks for detection of glyphosate herbicide in vegetables extract. *Microchem. J.* **2025**, *208*, 112407. DOI
103. Biswas, S.; Naskar, H.; Pradhan, S.; Wang, Y.; Bandyopadhyay, R.; Pramanik, P. Simultaneous voltammetric determination of Adrenaline and Tyrosine in real samples by neodymium oxide nanoparticles grafted graphene. *Talanta* **2020**, *206*, 120176. DOI
104. Mulik, B. B.; Munde, A. V.; Dighole, R. P.; Sathe, B. R. Electrochemical determination of semicarbazide on cobalt oxide nanoparticles: implication towards environmental monitoring. *J. Environ. Chem. Eng.* **2021**, *93*, 259-66. DOI
105. Narayanan, M.; Singh Chauhan, N. P.; Perumal, P. A highly efficient metal oxide incorporated metal organic framework [Nd_2O_3-MIL(Fe)-88A] for the electrochemical detection of dichlorvos. *RSC. Adv.* **2023**, *13*, 5565-75. DOI PubMed PMC
106. Tao, L.; Liu, X.; Tan, H.; Song, J.; Wei, J.; Zhu, C. Reliable ratiometric electrochemical sensor for methyl parathion detection in vegetables based on Nile blue A-functionalized Ce-MOF/carbon nanohorns composite. *Food. Chem.* **2026**, *508*, 148343. DOI
107. Guan, H.; Wang, N.; Feng, X.; Bian, S.; Li, W.; Chen, Y. FeMn bimetallic MOF directly applicable as an efficient electrocatalyst for overall water splitting. *Colloid. Surface. A.* **2021**, *624*, 126596. DOI
108. Sivasubramaniyan, S. M.; Suresh, I.; Balasubramanian, S.; Nesakumar, N.; Rayappan, J. B. B.; Kulandaisamy, A. J. Electrochemical detection of profenofos in water using a UiO-67 metal organic framework with graphene oxide composite. *Anal. Methods.* **2025**, *17*, 4190-205. DOI
109. Janjani, P.; Bhardwaj, U.; Agarwal, M.; Gupta, R.; Kushwaha, H. S. MIL-88B(Fe) MOF modified screen-printed electrodes for non-enzymatic electrochemical sensing of malathion. *Environ. Technol.* **2023**, *45*, 2649-59. DOI
110. Zhao, W.; Lu, J.; Chen, H.; et al. Advance in organophosphorus pesticides detection technology based on acetylcholinesterase inhibition. *Process. Saf. Environ. Prot.* **2025**, *203*, 107846. DOI
111. Zhang, Q.; Yu, J.; Wei, Y.; et al. Advances in acetylcholinesterase-based biosensing technologies for organophosphorus pesticide detection: a comprehensive review (2020-2024). *Food. Chem.* **2025**, *496*, 146769. DOI
112. Song, Y.; Chen, J.; Sun, M.; et al. A simple electrochemical biosensor based on AuNPs/MPS/Au electrode sensing layer for monitoring carbamate pesticides in real samples. *J. Hazard. Mater.* **2016**, *304*, 103-9. DOI
113. Wang, X.; Yang, S.; Shan, J.; Bai, X. Novel electrochemical acetylcholinesterase biosensor based on core-shell covalent organic framework@multi-walled carbon nanotubes (COF@MWCNTs) composite for detection of malathion. *Int. J. Electrochem. Sci.* **2022**, *17*, 220543. DOI
114. Yang, K.; Zhao, H.; Li, N.; et al. Facile synthesis of novel porphyrin-based covalent organic frameworks integrated with Au nanoparticles for highly sensitive detection of organophosphorus pesticide residues. *Microchem. J.* **2024**, *203*, 110945. DOI
115. Mahmoudi, E.; Fakhri, H.; Hajian, A.; Afkhami, A.; Bagheri, H. High-performance electrochemical enzyme sensor for organophosphate pesticide detection using modified metal-organic framework sensing platforms. *Bioelectrochemistry* **2019**, *130*, 107348. DOI
116. Hosseini, M.; Sadat Sabet, F.; Khabbaz, H.; Aghazadeh, M.; Mizani, F.; Ganjali, M. R. Enhancement of the peroxidase-like activity of cerium-doped ferrite nanoparticles for colorimetric detection of H_2O_2 and glucose. *Anal. Methods.* **2017**, *9*, 3519-24. DOI
117. Liu, F.; Liang, Z.; Zhang, Y.; et al. Evaluation of the potential application of RAPA-based delivery: Structural evolution and biocompatibility of monodispersed nano-ZIF-8@RAPA. *Mater. Today. Commun.* **2025**, *47*, 113163. DOI
118. Wen, L.; Wang, N.; Liu, Z.; et al. Acetylcholinesterase immobilization on ZIF-8/graphene composite engenders high sensitivity electrochemical sensing for organophosphorus pesticides. *Chemosensors* **2022**, *10*, 418. DOI
119. Xue, Y.; Gao, R.; Lin, S.; Zhong, Q.; Zhang, Q.; Hong, J. Regulating the interface electron distribution of iron-based MOFs through ligand functionalization enables efficient peroxymonosulfate utilization and catalytic performance. *J. Colloid. Interface. Sci.* **2024**, *663*, 358-68. DOI
120. Liu, Y.; Zhou, M.; Jin, C.; et al. Preparation of a sensor based on biomass porous carbon/covalent-organic frame composites for pesticide residues detection. *Front. Chem.* **2020**, *8*, 643. DOI PubMed PMC
121. Chansi, .; R., P. R.; Mukherjee, I.; Basu, T.; Bharadwaj, L. M. Metal organic framework steered electrosynthesis of anisotropic gold nanorods for specific sensing of organophosphate pesticides in vegetables collected from the field. *Nanoscale* **2020**, *12*, 21719-33. DOI
122. Wen, S.; Zhang, H.; Yu, S.; Ma, J.; Zhu, J.; Zhou, Y. Complementary homogeneous electrochemical and photothermal dual-modal sensor for highly sensitive detection of organophosphorus pesticides via stimuli-responsive COF/methylene blue@MnO_2 composite. *Anal. Chem.* **2023**, *95*, 14914-24. DOI
123. Zhao, F.; Liu, Y.; Lan, J. One-step electrosynthesis of Cu-Hemin MOFs/CNTs for the dual determination of glyphosate. *Microchim. Acta.* **2024**, *191*, 564. DOI

124. Liu, Y.; Wang, L.; Li, H.; et al. Rigorous recognition mode analysis of molecularly imprinted polymers - rational design, challenges, and opportunities. *Prog. Polym. Sci.* **2024**, *150*, 101790. DOI
125. Zhong, Y.; Li, Z.; Zhang, A.; et al. A molecularly imprinted electrochemical sensor MIP/Cu-MOF/rGO/AuNPs/GCE for highly sensitive detection of electroneutral organophosphorus pesticide residues. *Microchim. Acta.* **2024**, *191*, 338. DOI
126. Ma, X.; Kang, J.; Wu, Y.; et al. A bifunctional polycentric-affinity MOF/MXene heterojunction-based molecularly imprinted photoelectrochemical organophosphorus-sensing platform. *Chem. Eng. J.* **2023**, *469*, 143888. DOI
127. Yu, L.; Chen, X.; Yuan, M.; et al. MIPs and aptamer-based dual-recognition electrochemical sensor utilizing PtAuNPs functionalized Kagome COFs for ultrasensitive chlorpyrifos detection. *J. Alloys. Compd.* **2025**, *1041*, 183776. DOI
128. Fan, Y.; Li, J.; Amin, K.; et al. Advances in aptamers, and application of mycotoxins detection: a review. *Food. Res. Int.* **2023**, *170*, 113022. DOI
129. Dong, J.; Wang, G.; Geng, L.; et al. Electrochemical aptamer sensor based on bimetallic CuZr-MOF and AuNPs for ultrasensitive detection of organophosphorus pesticides in vegetables. *J. Food. Compos. Anal.* **2025**, *144*, 107761. DOI
130. Yiwei, X.; Xupeng, J.; Sennan, Y.; et al. An aptasensor with colorimetric and electrochemical dual-outputs for malathion detection utilizing peroxidase-like activity of Fe-MOF. *Food. Chemistry:. X.* **2024**, *24*, 101835. DOI PubMed PMC
131. Long, Y.; Bao, L.; Peng, Y.; Zhang, Z.; Pang, D. Self-co-reactant and ion-annihilation electrogenerated chemiluminescence of carbon nanodots. *Carbon* **2018**, *129*, 168-74. DOI
132. Han, D.; Yang, K.; Sun, S.; Wen, J. Signal amplification strategies in electrochemiluminescence biosensors. *Chem. Eng. J.* **2023**, *476*, 146688. DOI
133. Zhang, W.; Wu, J.; Shi, W.; et al. New function of metal-organic framework: structurally ordered metal promoter. *Adv. Mater.* **2023**, *35*, 2303216. DOI
134. Gu, C.; Ji, S.; Chen, Z.; et al. Enrichment-catalytic synergistically enhanced electrochemiluminescence sensors based on IRMOF-3/CdTe for ultrasensitive detection of organophosphorus pesticides. *Biosens. Bioelectron.* **2025**, *279*, 117398. DOI
135. Shen, Z.; Xu, R.; Wang, G.; et al. Self-luminescent dual-ligand metal-organic framework based electrochemiluminescence probes for organophosphorus pesticides determination. *Food. Chem.* **2025**, *478*, 143679. DOI